STRUCTURAL FRAMEWORK OF THE FRIES FAULT ZONE SOUTH OF RINER, VIRGINIA

by

Richard Sawyer Whitmarsh

Thesis submitted to the Faculty of the

Virginia Polytechnic Institute and State University

in partial fulfillment of the requirements for the degree of

MASTER OF SCIENCE

in

Geological Sciences

APPROVED:

Richard D. Law

R.D. Law, Chairman

Lynn Glover III

L. Glover, III

R.J. Tracy

November, 1994
Blacksburg, Virginia

STRUCTURAL FRAMEWORK OF THE FRIES FAULT ZONE SOUTH OF RINER, VIRGINIA

by

Richard Sawyer Whitmarsh

Committee Chairman: R.D. Law

Geological Sciences

(ABSTRACT)

The Fries fault zone south of Riner, Virginia is marked by a ductile, greenschist-facies thrust that places Middle Proterozoic gneiss over deformed Late Proterozoic(?)–Early Paleozoic rocks of the western Blue Ridge province. This work presents an analysis of the field relationships and finite strain patterns within the fault zone, and further relates these features to an interpretation of its structural framework. A geologic map of the fault zone is provided, in addition to more detailed lithologic descriptions within the text. Noteworthy aspects of the field geology include: (1) the discovery of a reasonable protolith to the mylonitic Little River Gneiss, which could previously only be inferred; and (2) the recognition of a varied lithologic assemblage that is considered to be correlative with the Pilot Gneiss, which is exposed along strike within the Brush Creek anticlinorium.

Kinematic analysis of tectonic fabrics within the Little River Gneiss, Pilot Gneiss, and Chilhowee Group suggest that the fault zone developed in response to southeast–northwest shortening, accomodated by general noncoaxial flow, which produced a top-to-the-northwest sense of shear at all scales of observation. However, it is evident that the original stratigraphic anisotropy within the Chilhowee Group effectively partitioned the coaxial and noncoaxial components of strain. Additional finite strain analyses within the Chilhowee Group, including the correlation of $R_f/\emptyset$ data with quartz *c*-axis fabrics, indicate that there is considerable variation in the geometry of finite strain along the fault

zone. Whereas flattening strains appear to predominate, it is evident that domains of constrictional strain and plane strain are localized near the nose of the Brush Creek anticlinorium.

These data are considered to support an interpretation in which the Pilot Gneiss and Chilhowee Group were metamorphosed and folded into a doubly-plunging antiform during the Taconic orogeny (*ca.* 480-435 Ma), and that progressive shortening of the Laurentian continental margin during this interval caused the Little River Gneiss to be uplifted along the Fries fault. The present structural framework of the Fries fault zone south of Riner, Virginia is thus considered to represent a northwest-vergent fold composed of Late Proterozoic–early Paleozoic strata, which is transected by the base of the Little River Gneiss.

ACKNOWLEDGEMENTS

Many thanks are due the individuals and organizations who contributed to the completion of this thesis. Foremost of these are the Faculty and Staff of the Department of Geological Sciences at Virginia Tech, who provided endless logistical support ranging from fieldwork to finishing. Special thanks to my advisor, Rick Law, for providing the intellectual seed for this project, as well as for his instruction and guidance during the research and completion of this thesis. Thanks also to Bob Tracy and Lynn Glover for their literary reviews, and for promoting my understanding and appreciation of Appalachian geology, north to south. In addition to these individuals, I owe an enormous amount of gratitude to the other members of the Faculty, their associates, and their students who participated in any of the field trips, seminars, or late night discussions where old ideas were criticized and new ideas were born. This research was supported directly by grants from the Geological Society of America, Sigma Xi, and the Appalachian Basin Industrial Associates. Additional support was obtained from British Petroleum through their Summer Intern Programs in Anchorage and Houston.

TABLE OF CONTENTS

TABLE OF CONTENTS
(continued)

TABLE OF CONTENTS
(continued)

LIST OF FIGURES

LIST OF FIGURES
(continued)

LIST OF TABLES

LIST OF APPENDICES

LIST OF PLATES
(items located in pocket at back of thesis)

CHAPTER ONE:

BACKGROUND

1.1 Introduction

The Fries fault zone is widely recognized as one of several prominent ductile-deformation zones within the Blue Ridge Province of the central and southern Appalachians (Figure 1). It is also considered by some investigators to have been an important, if not fundamental, crustal structure during both late Proterozoic extension and subsequent Paleozoic contraction (Wehr & Glover 1985, Simpson & Kalaghan 1989). Even prior to these studies, however, the importance of the Fries, Rockfish Valley, and Hayesville fault systems (Figure 1) had been realized as they were interpreted to separate distinct metamorphic and plutonic terranes during the Grenville and Taconic orogenies (Bartholomew & Lewis 1984, Hatcher & Odom 1980). The fundamental nature of the Fries fault zone is underscored, as well, by the recognition of multiple thermal (Dietrich *et al.* 1969, Hatcher 1978) and deformational events (Kaygi 1979) during the Paleozoic.

This investigation is based upon more recent work in which the Fries fault zone is considered to represent a thrust-reactivated structure of the Laurentian rifted margin (*e.g.* Wehr & Glover 1985). Given this hypothesis, it is reasonable that one may expect to observe remnants of the structures and/or stratigraphy related to late Proterozoic extension within the fault zone. However, recent work along the Rockfish Valley fault zone indicates that extensional deformation was localized to the east of, rather than along, this structure (Bailey & Simpson 1993). Therefore, a concentrated analysis of the field relations and strain patterns within the Fries fault zone was conducted in order to: first, establish the presence or absence of these late Proterozoic extensional components and,

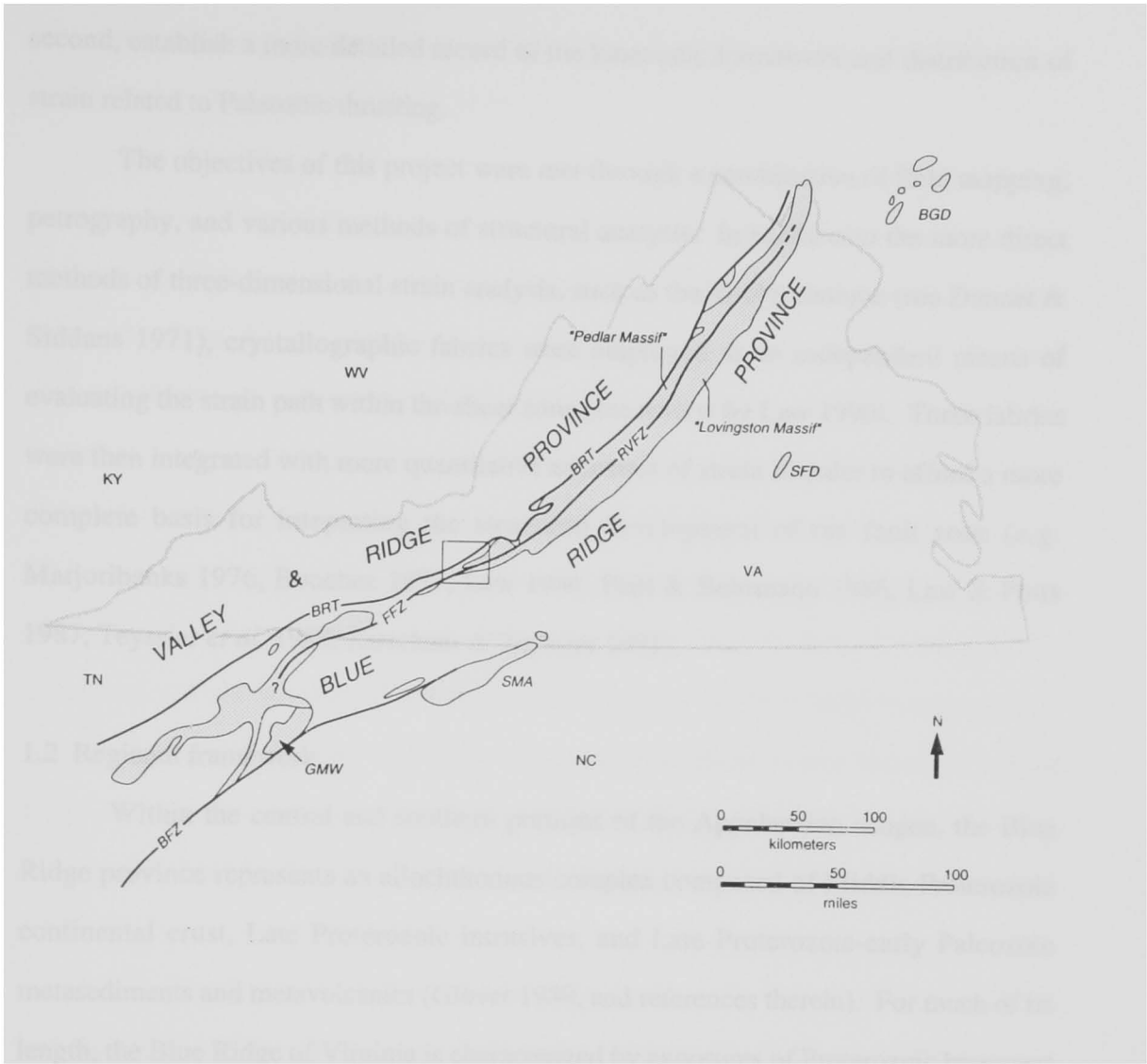

Figure 1. Generalized distribution of Proterozoic basement (stippled) and location of several major tectonic boundaries within the central and southern Appalachians; Virginia state boundary indicated by stippled outline. BFZ, Brevard fault zone; BGD, Baltimore gneiss domes; BRT, Blue Ridge thrust; FFZ, Fries fault zone; GMW, Grandfather Mountain window; RVFZ, Rockfish Valley fault zone; SFD, State Farm dome; SMA, Sauratown Mountains anticlinorium. Box indicates approximate location of Figure 2. Adapted from Bartholomew & Lewis (1984).

second, establish a more detailed record of the kinematic framework and distribution of strain related to Paleozoic thrusting.

The objectives of this project were met through a combination of field mapping, petrography, and various methods of structural analysis. In addition to the more direct methods of three-dimensional strain analysis, such as the $R_f/\emptyset$ technique (see Dunnet & Siddans 1971), crystallographic fabrics were employed as an independent means of evaluating the strain path within the shear zone (see review by Law 1990). These fabrics were then integrated with more quantitative estimates of strain in order to afford a more complete basis for intepreting the structural development of the fault zone (*e.g.* Marjoribanks 1976, Bouchez 1977, Law 1986, Platt & Behrmann 1986, Law & Potts 1987, Teyssier *et al.* 1988, Kirschner & Teyssier 1991).

1.2 Regional framework

Within the central and southern portions of the Appalachian orogen, the Blue Ridge province represents an allochthonous complex composed of Middle Proterozoic continental crust, Late Proterozoic intrusives, and Late Proterozoic-early Paleozoic metasediments and metavolcanics (Glover 1989, and references therein). For much of its length, the Blue Ridge of Virginia is characterized by exposures of Proterozoic basement flanked by metamorphosed strata which define the Blue Ridge anticlinorium (Figure 1). Within this, Bartholomew *et al.* (1981) had interpreted two distinct metamorphic terranes, or "massifs", which are juxtaposed along the Fries and Rockfish Valley fault zones (Figure 1). However, more recent work by Evans (1991) and Bailey & Simpson (1993) suggests that the Lovingston and Pedlar massifs are distinguished only on the basis of a selective amphibolite-facies overprint of granulites within the Lovingston massif, and that

"there was not a significant amount of thrust displacement on the Rockfish Valley fault zone" (Bailey & Simpson 1993, p. 421).

The Blue Ridge cover sequence includes a variety of clastic, volcanic, and intrusive units of variable continuity which were probably deposited successive to late Proterozoic extension of the continental margin (*e.g.* figure 8 in Glover 1989). Since then, the Blue Ridge allochthon has experienced several periods of regional metamorphism and deformation (Glover *et al.* 1983, Bartholomew & Lewis 1984) prior to its final emplacement along the Blue Ridge thrust (Figure 1). Initial uplift of the Blue Ridge during the Taconic orogeny is indicated by synorogenic conglomerates of Late Ordovician age (Karpa 1974), although it can only be speculated that the Rockfish Valley and Fries fault zones may have localized some of this uplift (as in Wehr & Glover 1985). In its present state, however, the allochthonous nature of the Blue Ridge is supported by seismic data which indicate that lower Paleozoic shelf strata extend beneath the Blue Ridge for approximately 45 km southeast of the Blue Ridge structural front before being truncated at depth by the Blue Ridge thrust (Lampshire *et al.* 1994, see also Cook *et al.* 1979).

The Blue Ridge thrust marks the boundary between the Valley & Ridge province and the overthrust Blue Ridge province (Figures 1 and 2). The Valley & Ridge province itself is characterized by dominantly northwest-vergent structures involving Paleozoic strata which compose the foreland fold-and-thrust belt of the Appalachian orogen. Similar southeast-northwest contraction is evident along the Blue Ridge thrust, where greenschist-facies rocks of the Blue Ridge complex are thrust over virtually unmetamorphosed shelf strata. Deformation along this contact is characteristically brittle, although a well-developed cleavage is commonly observed within the less competent units located immediately beneath the thrust surface. In contrast, fault zones within the

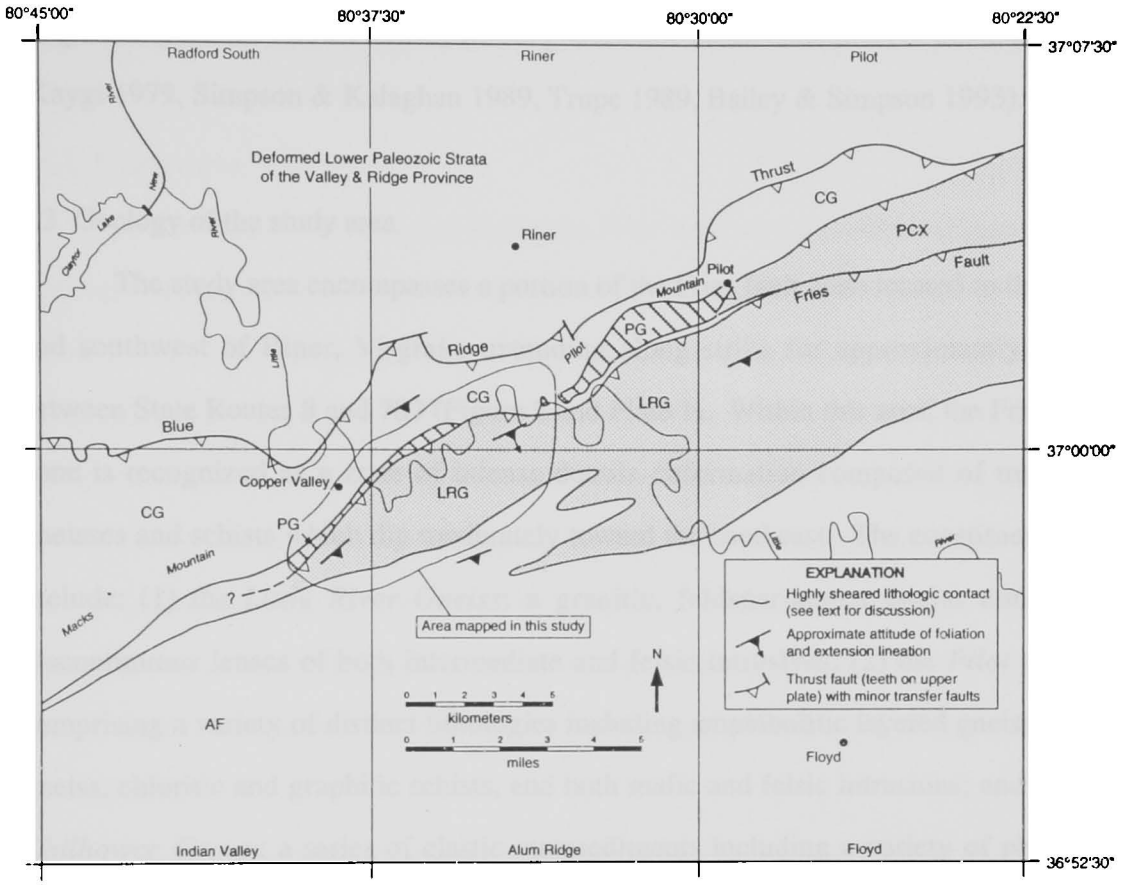

CG: Chilhowee Group (Cambrian); metasediments including quartz arenites, feldpathic sandstones, siltstones, and rare calcareous breccias. Well-foliated near contacts with Pilot Gneiss (PG) and Little River Gneiss (LRG).

AF: Ashe Formation (Precambrian); predominantly biotite-quartz-feldspar schists with few exposures of muscovite phyllite.

PG: Pilot Gneiss (Precambrian); includes chlorite-epidote-actinolite schists and layered gneisses with lesser amounts of leucocratic gneiss, mafic dikes/sills, graphitic schist, and rare garnetiferous tectonite. Mylonitic textures predominate.

LRG: Little River Gneiss (Precambrian, *ca.* 1128 Ma); feldspar-augen gneiss, exhibits varying degrees of mylonitization, locally ultramylonitic at base. Includes rare exposures of garnet-bearing porphyroblastic gneiss oriented at a high angle to the dominant fabric.

PCX: Precambrian granoblastic gneiss of uncertain affinity.

Figure 2. Generalized geologic map of the Fries fault zone in southwestern Virginia (refer to Figure 1) including the approximate limits of the area mapped in this study. Compiled and adapted from Bartholomew & Lewis (1984), Dietrich (1954, 1959), Kaygi (1979), Lewis (1975), McDowell (1968), and Truman (1976).

Blue Ridge province—such as the Fries fault zone—are characterized by higher-temperature, ductile fabrics formed within greenschist-facies conditions of metamorphism (Kaygi 1979, Simpson & Kalaghan 1989, Trupe 1989, Bailey & Simpson 1993).

1.3 Geology of the study area

The study area encompasses a portion of the Fries fault zone located to the south and southwest of Riner, Virginia, extending along strike for approximately 10 km between State Routes 8 and 787 (Figure 2 and Plate 1). Within this area, the Fries fault zone is recognized as a zone of intense ductile deformation composed of mylonitic gneisses and schists which dip moderately toward the southeast. The constituent units include: (1) the *Little River Gneiss*: a granitic, feldspar-augen gneiss containing discontinuous lenses of both intermediate and felsic intrusives; (2) the *Pilot Gneiss*: comprising a variety of distinct lithologies including amphibolitic layered gneiss, felsic gneiss, chloritic and graphitic schists, and both mafic and felsic intrusions; and (3) the *Chilhowee Group*: a series of clastic metasediments including a variety of phyllites, schists, quartzites, and lithic conglomerates. These units are exposed discontinuously along strike for the length of the study area, although their structural interrelationships are best observed in the southwestern portion of the mapped area—near Copper Valley, along the Indian Creek drainage.

1.4 Previous work

The gross structural and stratigraphic relationships within this portion of the Fries fault zone were first described by Dietrich (1954, 1959) who covered a large portion of the area illustrated in Figure 2. This region has since been the focus of several more

detailed investigations concerning the stratigraphy, structure, and geochronology of units both within, and adjacent to, the area mapped in this study (see Figures 2 and 3).

1.4.1 Stratigraphic interpretations

Intense ductile deformation within the Fries fault zone has obscured many of the lithologic characteristics necessary for proper stratigraphic assignment of tectonites within the fault zone. This is particularly evident within the Chilhowee Group where, even though the units may be confidently identified as metasedimentary, their position within the Chilhowee Group stratigraphy is quite uncertain. At the other extreme, it is tempting to ascribe the compositional layering within the Pilot Gneiss to a metasedimentary protolith, although such an interpretation is highly speculative at this stage. The Little River Gneiss, on the other hand, is widely accepted as a part of the Grenville plutonic suite which is recognized throughout the Blue Ridge province (see Bartholomew & Lewis 1984).

The metasedimentary units presently assigned to the Chilhowee Group (Figure 2 and Plate 1) were first described by Dietrich (1954) as lithologic equivalents to the Unicoi and Hampton formations of the Chilhowee Group exposed elsewhere in the southern Appalachians. A number of subsequent studies in the area have also recognized a strongly folded Chilhowee Group stratigraphy (*e.g.* Dietrich 1959, McDowell 1968, Truman 1976, Kaygi 1979). However, intensely deformed sections within the fault zone have previously been correlated with the late Precambrian Ashe Formation which overlies Grenville basement rocks to the south and west (Rankin *et al.* 1973, Lewis 1975).

During the initial mapping of the region, the Pilot Gneiss (Figure 2 and Plate 1) had been included as part of the Precambrian basement complex (Dietrich 1954, 1959, McDowell 1968, Rankin *et al.* 1973). Lewis (1975) later recognized similar units near

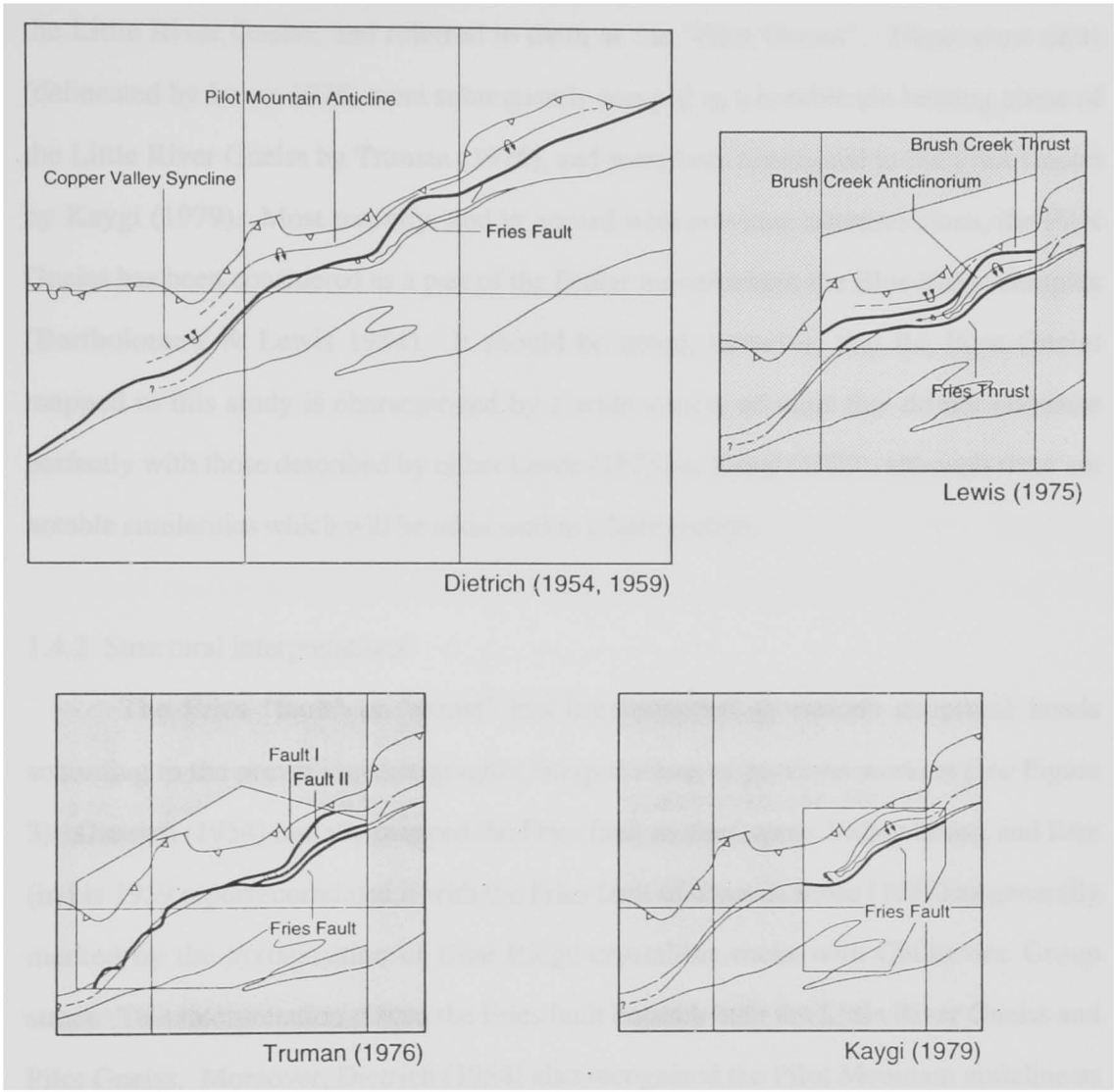

Figure 3. Previous interpretations concerning the structure of the Fries fault zone. Base map contains contacts shown in Figure 2.

the town of Pilot, Virginia, although lithologically distinct and structurally isolated from the Little River Gneiss, and referred to them as the "Pilot Gneiss". These same units (delineated by Lewis 1975) were subsequently mapped as a hornblende-bearing phase of the Little River Gneiss by Truman (1976), and were later reassigned to the Pilot Gneiss by Kaygi (1979). Most recently, and in accord with previous interpretations, the Pilot Gneiss has been considered as a part of the Pedlar massif within the Blue Ridge complex (Bartholomew & Lewis 1984). It should be noted, however, that the Pilot Gneiss mapped in this study is characterized by a wide variety of units that do not correlate perfectly with those described by either Lewis (1975) or Kaygi (1979), although there are notable similarities which will be addressed in a later section.

1.4.2 Structural interpretations

The Fries "fault" or "thrust" has been mapped at various structural levels according to the prevailing stratigraphic interpretations of previous workers (see Figure 3). Dietrich (1954) initially mapped the Fries fault as the Copper Valley thrust, and later (in his 1959 report) correlated it with the Fries fault of Stose & Stose (1957) as generally marked by the juxtaposition of Blue Ridge crystalline rocks with Chilhowee Group strata. This interpretation placed the Fries fault beneath both the Little River Gneiss and Pilot Gneiss. Moreover, Dietrich (1954) also recognized the Pilot Mountain anticline as the only major structure within the transition zone between the Fries fault and Blue Ridge thrust, noting that it consisted of intensely deformed Chilhowee Group metasediments exposed in a northwest-vergent, overturned anticline. McDowell (1968), as well, recognized several kilometer-scale, northwest-vergent folds within the Chilhowee Group where Dietrich (1959) had originally mapped the Copper Valley syncline.

Later, with the recognition of the Pilot Gneiss as a structurally separate unit defining the Brush Creek anticlinorium, Lewis (1975) reinterpreted the structure of Pilot Mountain as that of an overturned syncline located in the footwall of the overthrust anticlinorium. This interpretation was subsequently revised according to Truman's (1976) consideration that the Pilot Gneiss was a thrust-bounded slice of the Little River Gneiss. Most recently, however, the Fries "fault" has been placed at the base of the Little River Gneiss, with the Pilot Gneiss occupying the core of the Brush Creek anticlinorium (Kaygi 1979, Bartholomew & Lewis 1984, Bartholomew *pers. comm.* 1992). In addition, it is interesting to note that Kaygi (1979) depicts the axis of the Brush Creek anticlinorium to be sharply folded and apparently trucated by the Fries fault. The same temporal relation is implied from the independent results of this study as well (see discussion section).

Kaygi (1979) also identified as many as four phases of Paleozoic deformation interpreted to be the result of progressive simple shear and late-stage flattening within the fault zone. Among these stages is the development of the Pilot Gneiss "mega-nappe" in association with D1 prior to the retrograde metamorphism and mylonitization (D2) within the Fries fault zone. Furthermore, the deformational history outlined by Kaygi (1979) is consistent with progressive northwest-vergent contraction at various times during the Paleozoic. However, with more recent advances in structural petrology and kinematic analysis of shear zones (*e.g.* Berthé *et al.* 1979a, 1979b, White *et al.* 1980, Lister & Williams 1979, Lister & Snoke 1984, Passchier & Simpson 1986, Hanmer & Passchier 1991, and many others), it has been become apparent that mylonites along correlative strands of the Fries fault zone preserve evidence of extension as well as contraction (Simpson & Kalaghan 1989).

1.4.3 Geochronologic studies

The Little River Gneiss was initially dated by Dietrich *et al.* (1969) who reported an Rb-Sr whole-rock age of 1320 ±100 Ma outside of the fault zone, while K-Ar and Rb-Sr analyses of biotite and feldspar separates from within the fault zone yielded ages of approximately 350 ±40 Ma. These younger ages were recognized to fall within the range of those defining the Acadian orogeny, although a firm correlation was only speculated. Fullagar & Odom (1973) later reported an Rb-Sr age of 1174 ±14 Ma for the Grayson Gneiss (approx. 100 km to the southwest), and inferred the Little River Gneiss to be of similar age with a higher initial $^{87}Sr/^{86}Sr$ ratio. Using this Rb-Sr data, Truman (1976) calculated an average age for the Little River Gneiss of 1185 ±231 Ma, and further reported a U-Pb (zircon) age of 1128 ±25 Ma which is presently accepted as the age of igneous emplacement. The Little River Gneiss is therefore considered to represent one of many units within the Blue Ridge province which define the age of plutonic activity (*ca.* 1050-1150 Ma) during the Grenville orogeny (Bartholomew & Lewis 1984). The precise age of mylonitization (*ca.* 350 Ma ?) remains to be determined.

Dietrich *et al.* (1969) also reported several whole-rock ages for samples of "sheared 'older Precambrian gneiss'" from within the fault zone. However, two of these were apparently collected from sites which are now considered to be a part of the Pilot Gneiss. Their sample #128 is most certainly from within the Pilot Gneiss and has yielded ages of 345 ±17 Ma (K-Ar) and 460 Ma (Rb-Sr). The younger K-Ar age may be attributed to the same "Acadian" event (*ca.* 350 Ma) which affected the Little River Gneiss. On the other hand, the Rb-Sr age is significantly older and may represent Taconic metamorphism (*ca.* 480-435 Ma, Glover *et al.* 1983). Another of their samples (#238) may have been obtained from the Pilot Gneiss near Copper Valley (although this is far less certain) and also yielded a peculiar Rb-Sr age of 585 Ma. The significance of

these ages with respect to the Pilot Gneiss will be treated further in the discussion section.

CHAPTER TWO:

LITHOLOGIC DESCRIPTIONS

2.1 Little River Gneiss

The Little River Gneiss is generally referred to as a granitic, feldpar-augen gneiss due to the dominance of that particular lithology throughout the area. However, several distinct phases of the gneiss have been recognized, including both equigranular and porphyroblastic phases, as well as the predominant augen gneiss—all of which exhibit variable degrees of mylonitization.

2.1.1 Mylonitic augen gneiss

The predominant lithology within the Little River Gneiss is a mylonitic augen gneiss of quartz monzonitic to quartz monzodioritic composition (Truman 1976) containing blue quartz and alkali feldspar porphyroclasts within a biotite-rich, quartzo-feldspathic matrix. The matrix also contains variable amounts of chlorite, muscovite/sericite, epidote/clinozoisite, and remnant garnet, with accessory phases including apatite and zircon. This assemblage has accordingly been interpreted to have formed under greenschist-facies metamorphic conditions (approx. 400 to 450°C) during mylonitization (Kaygi 1979). The mylonitic texture of the augen gneiss (Figure 4A) is pervasive, although gradational, with the most intense fabrics observed near the base of the unit, along what has been considered to represent the "Fries fault" (*cf.* figure 22 in Kaygi 1979). Within the shear zone, the augen gneiss is transformed into a porphyroclastic, quartz-ribbon mylonite (Figure 4B) characterized by similar mineralogy, an extreme reduction in grain size, and a conspicuous, down-dip extension lineation defined by

A.

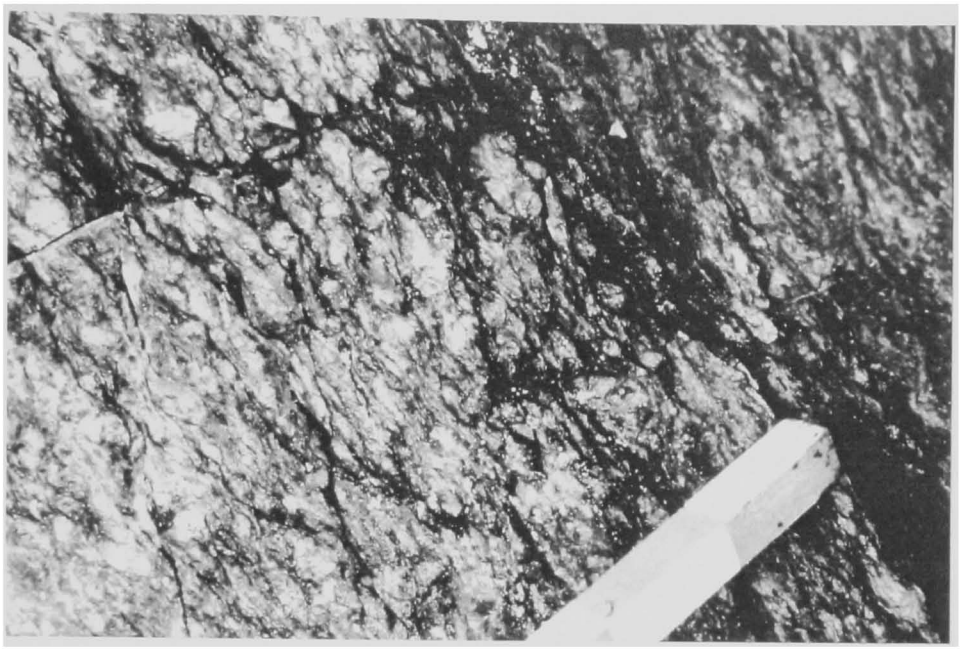

B.

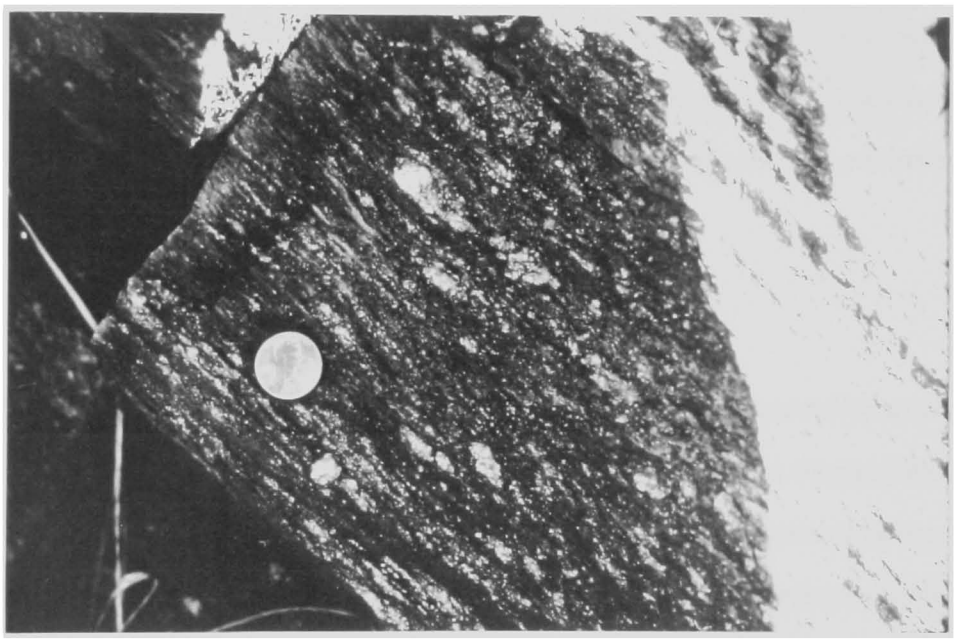

Figure 4. *Mylonitic textures within the Little River Gneiss.* **A.** Mylonitic augen gneiss exposed southwest of Copper Valley. Divisions on the staff are 10 cm in length. **B.** Quartz ribbon ultramylonite exposed at the base of the Little River Gneiss near Copper Valley. Note the dramatic reduction in grain size as compared to that in **A.** Coin is approximately 1.9 cm in diameter. Both viewed toward the northeast, see Appendix 1A for exact outcrop localities.

elongate quartz, feldspar, and phyllosilicate grains. Both alkali and plagioclase feldspar porphyroclasts are typically polycrystalline and exhibit relatively brittle behavior in contrast to the rather ductile deformation and recrystallization of quartz in the surrounding matrix (Figure 5). In some instances however, plagioclase does exhibit some evidence of intracrystalline slip (*e.g.* bent and kinked twin lamellae) which, in conjuction with the observed ductility in quartz, may be used to infer that the mylonitic fabrics were developed at temperatures in the range of 300 to 450°C (Tullis 1983).

Other phases of the Little River Gneiss are distinguished more on the basis of texture than mineralogy. One of these consists of a finer-grained equivalent of the augen gneiss which occurs sporadically throughout the area, possibly representing local high-strain zones within the formation. The other distinguishable phase is characterized by medium-grained leucocratic gneiss consisting of microcline and sodic plagioclase with subordinate amounts of recrystallized quartz and phyllosilicates. This phase is most prevalent in the south-central portion of the mapped area although it is not exclusive of the predominant augen gneiss.

2.1.2 Porphyroblastic gneiss

Another conspicuous phase of the Little River Gneiss is represented by a coarse-grained porphyroblastic gneiss composed of anhedral alkali feldspar megacrysts in a matrix of quartz, feldspar, garnet, biotite, and chlorite, along with accessory zircon and magnetite. The known exposures of this phase are limited to two locations within the central and western portions of the study area (see Plate 1). At both localities, foliation is subvertical and strikes within 5° of due north, and is defined by the apparent flattening of feldspar and chloritized garnet in addition to the preferential distribution of biotite within the pressure shadows adjacent to garnet porphyroblasts (Figure 6). Figure 7 illustrates

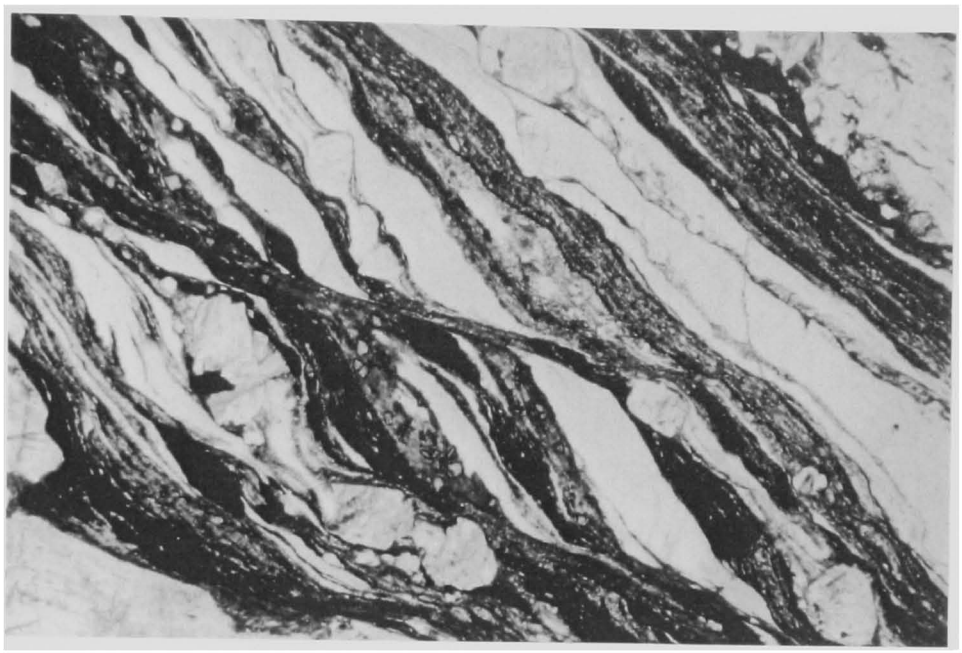

Figure 5. *Microtexture of Little River Gneiss ultramylonite.* The mylonitic foliation is characterized by abundant feldspar porphyroclasts within a matrix of quartz ribbons and phyllosilicate-rich domains. Grain size reduction is evident by the brittle fracture and segmentation of both garnet and feldspar within the more ductile matrix. Note remnant garnet fragments within chlorite near center of photo. Field of view is 6.5 mm in the long dimension, shot in plane-polarized light. Viewed toward the northeast in the same orientation as Figure 4B. Specimen FF-P4, see Appendix 1A for exact sample locality.

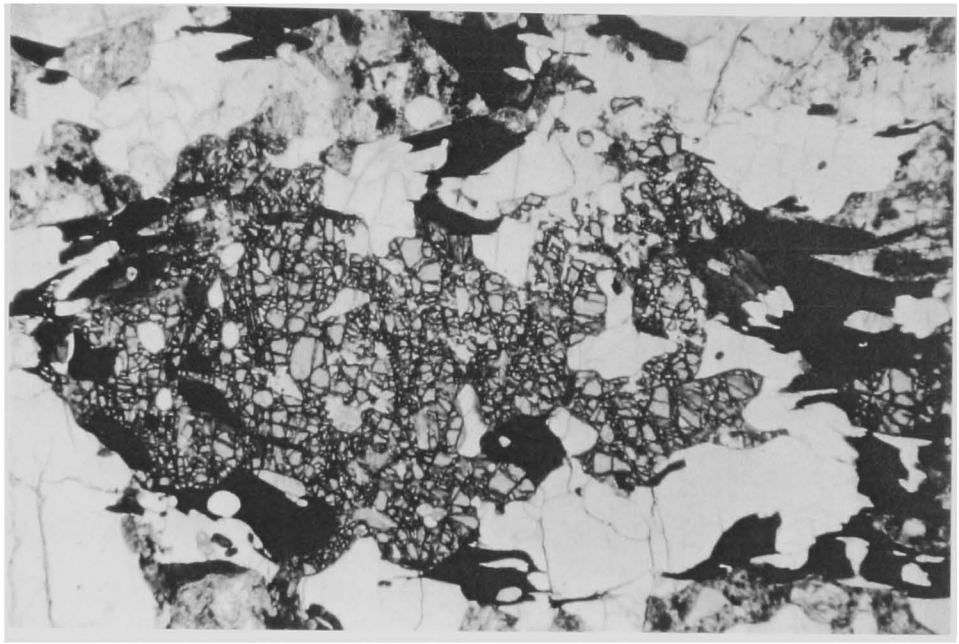

Figure 6. *Porphyroblastic texture of Little River Gneiss protolith.* Foliation (horizontal in photo, subvertical in field exposures) is well defined by chloritized garnet and biotite within a matrix of quartz and feldspar. Field of view is 6.5 mm in the long dimension, shot in plane-polarized light. Specimen FF-74, see Appendix 1A for exact locality.

the progressive transposition of this earlier fabric into the predominant mylonitic fabric along a traverse to the south of that exposure in the central portion of the study area. In this case, the progressive clockwise rotation and flattening has produced a fabric which is virtually parallel to the regional fabric. The petrology of the mylonitic augen gneiss further substantiates the interpretation that the garnet-bearing porphyroblastic gneiss is, in fact, the protolith to what is actually considered to be Little River Gneiss.

2.1.3 Dikes/sills

In addition to the various phases of the Little River Gneiss, discontinuous lenses of leucogranite and mafic dikes/sills have also been delineated within the basement (see Plate 1). Quartz+perthite leucogranites occur as massive, competent units (5 to 50 m thick) which lack the penetrative, southeast-dipping fabric observed within the Little River Gneiss. The mafic intrusives, on the other hand, are smaller in size (1 to 5 m thick), highly sheared, and composed of quartz, sodic plagioclase, blue-green hornblende, actinolite, biotite, chlorite, and epidote/clinozoisite. A concordant southeast-dipping foliation within these mafic units is well-defined by actinolite and chloritized biotite. Both of these units occur in linear arrays oriented subparallel to the regional fabric, and no clear crosscutting relationships among the two were observed during the course of this investigation. However, it may be speculated that these bodies represent dikes and/or sills which were intruded concurrently during late Precambrian rifting of the Laurentian continental margin, and that their present distribution simply reflects their transposition into the regional southeast-dipping fabric.

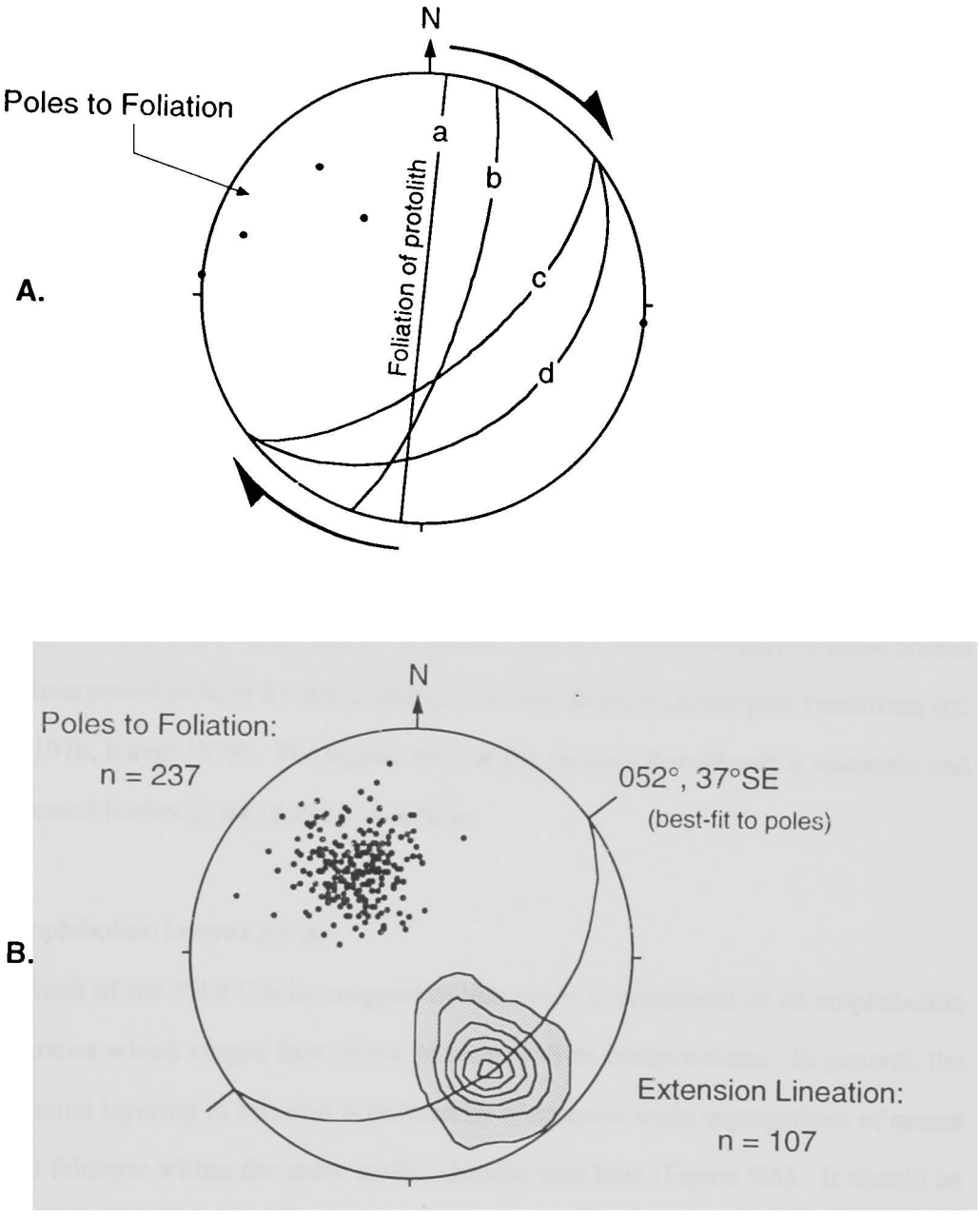

Figure 7. *Orientation of foliations and lineations within the study area.* **A.** Lower-hemisphere stereographic projections showing the orientation of the subvertical granoblastic foliation observed within the Little River Gneiss protolith and its progressive transposition (a-d) into the predominant mylonitic fabric observed within the study area, as depicted in **B.** Contours at 1, 5, 10, 15, 20, 25 times uniform.

2.2 Pilot Gneiss

Exposures of the Pilot Gneiss within the area of this investigation were first recognized and speculatively correlated to those within the Brush Creek anticlinorium by Kaygi (1979). This correlation is tentatively accepted, although the greater diversity of rock units within the Copper Valley area (Figure 2) precludes a rigorous correlation. The Pilot Gneiss mapped in this study is best characterized as a layered gneiss complex composed of chlorite-epidote-actinolite schists and gneisses which contain variable amounts of quartz, calcite, alkali feldspar, sodic plagioclase, and remnant hornblende. Fine-grained greenschists of this composition are intercalated with augen gneiss along the contact with the overlying Little River Gneiss (Figure 8). In addition, there are more distinct units within the Pilot Gneiss which are characterized by the presence of tremolite, muscovite, biotite, graphite, or garnet. Mylonitic textures defined in part by these phases are thus interpreted to have formed under greenschist-facies metamorphic conditions (*cf.* Truman 1976, Kaygi 1979). The significance of the remnant hornblende is uncertain and will be treated further in the discussion section.

2.2.1 Amphibolitic layered gneiss

Much of the Pilot Gneiss mapped in this study is composed of an amphibolitic layered gneiss which ranges from felsic to intermediate compositions. In general, the compositional layering in this unit is defined by centimeter-scale segregations of quartz and alkali feldspar within the more mafic, chlorite-rich host (Figure 9A). It should be noted, however, that both the scale and definition of the layering and the bulk composition of the ferromagnesian layers are quite variable. Alkali feldspar occurs in highly variable proportions and in places constitutes the majority of the rock, although it more commonly occurs as scattered porphyroclasts. Where hornblende is present, it

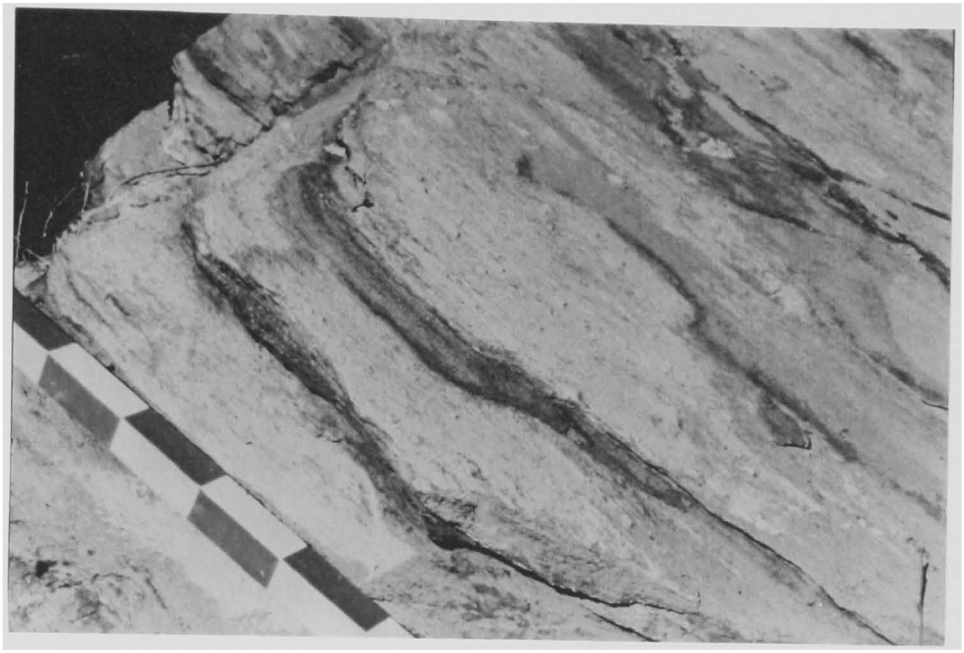

Figure 8. *Layered gneiss exposed along the Little River Gneiss/Pilot Gneiss contact.* The lighter layers are composed of feldspar augen gneiss with a well-developed extension lineation plunging down-dip, to the southeast (toward right in photo, parallel to staff). The darker layers consist of epidote-actinolite greenschists which may represent a portion of the underlying Pilot Gneiss. Divisions on the staff are 10 cm in length. Viewed toward the northeast, see Appendix 1A for exact outcrop locality.

A.

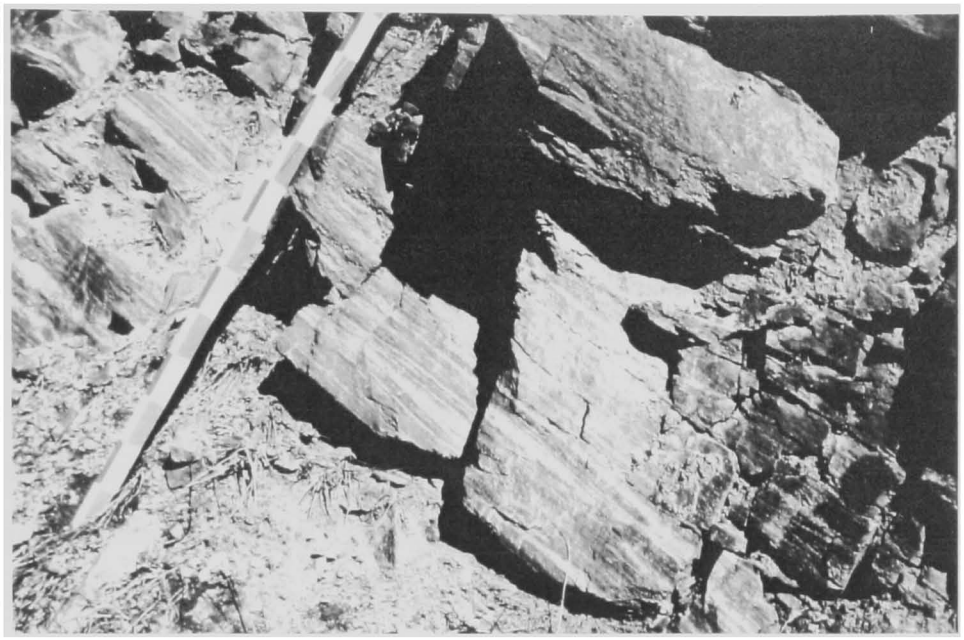

B.

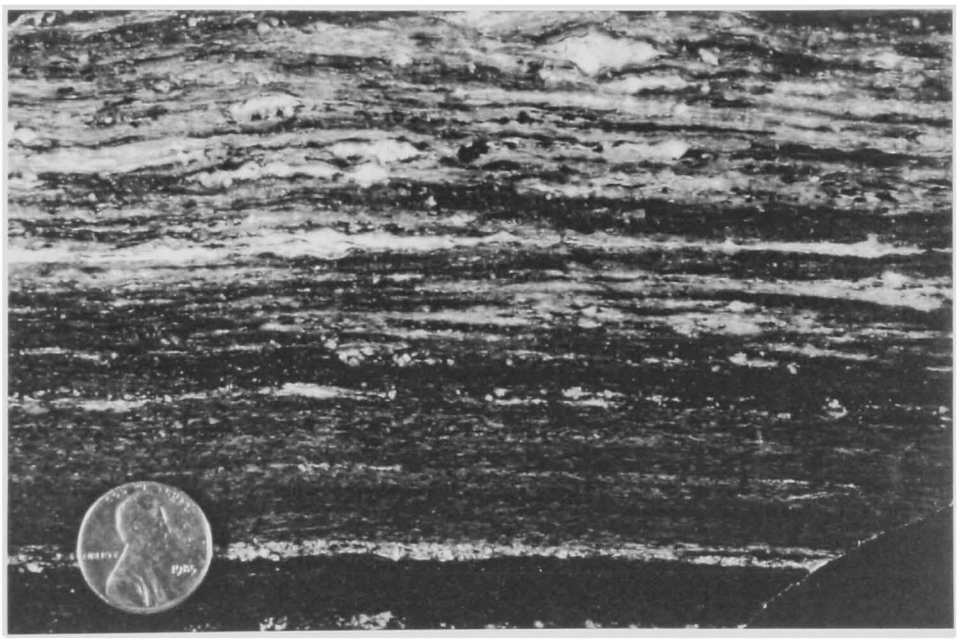

Figure 9. *Compositional layering within the Pilot Gneiss.* **A.** Amphibolitic layered gneiss exposed southwest of Copper Valley. Darker layers composed mainly of chlorite, epidote, actinolite, sodic plagioclase, and quartz; lighter layers consist of quartz and alkali feldspar. Divisions on staff are 10 cm in length. Viewed toward the northeast. **B.** Polished slab of same exposed southwest of Pilot. Remnant hornblende (dark) and alkali feldspar porphyroclasts (light) in mylonitic matrix. Coin is approx. 1.9 cm in diameter. Specimen in **B** is FF-130. See Appendix 1 for exact outcrop and sample localities.

(along with feldspar) is invariably porphyroclastic—occurring as relatively rigid grains within an otherwise ductile matrix of quartz, chlorite, and actinolite (Figures 9B and 10A). Porphyroclasts of actinolite (some cored by green-brown hornblende) are also common within this unit, and may indicate that a static greenschist-facies event preceded the dynamothermal metamorphism associated with mylonitization.

In contrast to the hornblende-rich granoblastic gneiss described by Kaygi (1979), the amphibolitic gneiss described here is dominated by mylonitic textures, and exposures of this particular lithology appear to be rare within the Brush Creek anticlinorium. A brief reconnaissance of the Brush Creek anticlinorium suggests that these mylonites (such as that in Figure 9B) are localized at the base of an overthrust granoblastic gneiss exposed near the town of Pilot. It is possible, therefore, that the amphibolitic layered gneiss mapped in this study is simply the mylonitized equivalent of a hornblende-bearing gneiss similar to that described by Kaygi (1979), although no relict granoblastic textures were observed within the layered gneiss.

2.2.2 Felsic gneiss

The Pilot Gneiss is further characterized by exposures of light-grey felsic gneiss (*e.g.* site 1 on Plate 1, also Appendix 1A) composed mainly of quartz and feldspar, with relatively minor amounts of muscovite and chlorite. Outcrops exhibit a rather massive texture in contrast to that observed in thin section where the foliation is well-defined by single-crystal quartz ribbons and phyllosilicates which envelop more rigid feldspathic pophyroclasts (Figure 10B). A determination of the protolith is difficult for this unit, although the presence of these components within a matrix of chlorite and muscovite may indicate a metasedimentary origin. This assemblage of phases may also be used to infer that metamorphic conditions were within the greenschist facies.

2.2.3 Chloritic schist

Chloritic schists are relatively abundant near the base of the Pilot Gneiss. These are typically composed of chlorite, chloritized biotite, calcite, and quartz, as well as variable amounts of actinolite, epidote, and sodic plagioclase. No remnant hornblende was observed in these samples, although their constituent mineralogy suggests that these schists may have been derived through progressive retrograde metamorphism of the amphibolitic layered gneiss or some compositionally equivalent lithology.

2.2.4 Graphitic schist

Graphite-bearing units were noted in a series of exposures near Copper Valley, which transect the overall northeasterly trend of the Pilot Gneiss. At the base of the Pilot Gneiss (site 2 on Plate 1, also Appendix 1A), graphite occurs as flakes which define the extension lineation within mylonitic schists composed of muscovite, tremolite, and quartz, with accessory rutile(?) and titanite. From this point on the map, units of similar composition, but varying texture, may be traced discontinuously upslope. Farther south, on State Route 619 (see Plate 1), a similar assemblage is observed within a rather massive, pale orange to brown-colored exposure (FF92 on Appendix 1A). Here, the graphite coexists with tremolite, muscovite, and biotite, in a matrix of plagioclase and quartz (Figure 10C). Foliation of this unit is poorly defined by graphite as well as the phyllosilicates, although the rock is essentially unfoliated in comparison to the surrounding units. The metamorphic mineralogy of these samples is suggestive of a calcareous metasedimentary protolith, perhaps an immature calcareous sandstone.

Graphite also occurs within a foliated intrusive(?) unit exposed near the base of the Little River Gneiss (refer to Plate 1). This exposure is characterized by coarse-grained, milky white to grey leucogranite in which the feldspar is pervasively altered.

A.

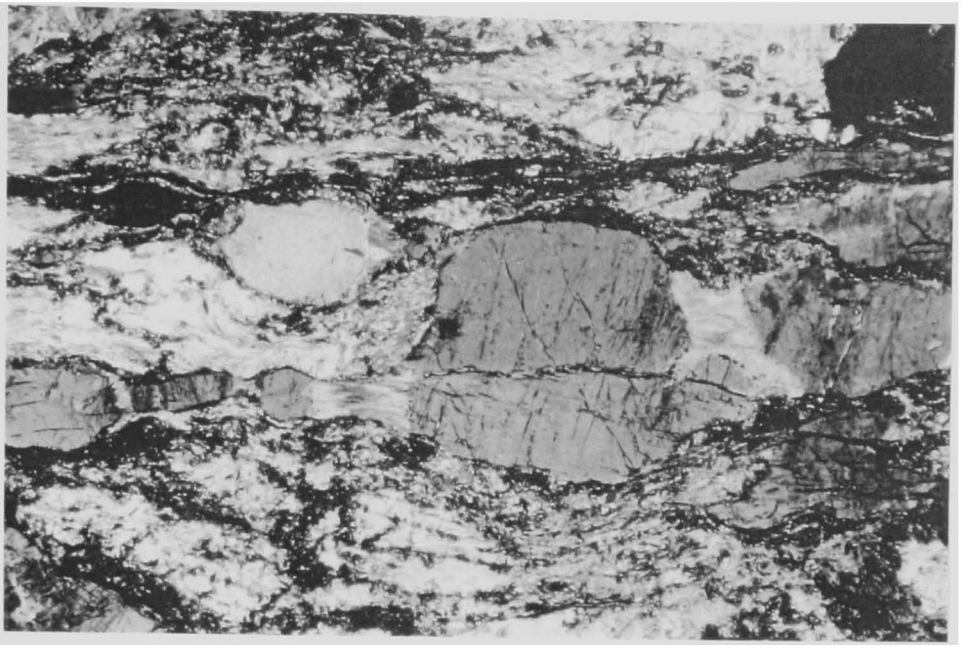

B.

Figure 10. *Mineral assemblages and textures within the Pilot Gneiss.* **A.** Actinolite and chlorite within pressure shadows of hornblende porphyroclasts indicates greenschist-facies conditions of deformation. Field of view is 6.5 mm in long dimension, plane-polarized light. Specimen FF-23. **B.** Felsic gneiss: foliation defined by quartz ribbons and mica-rich folia that envelop polycrystalline, feldspathic porphyroclasts. Field of view is 6.5 mm in long dimension, shot in partial-cross-polarized light. Specimen FF-35. Both oriented parallel to the local lineation, see Appendix 1A for exact sample localities.

C.

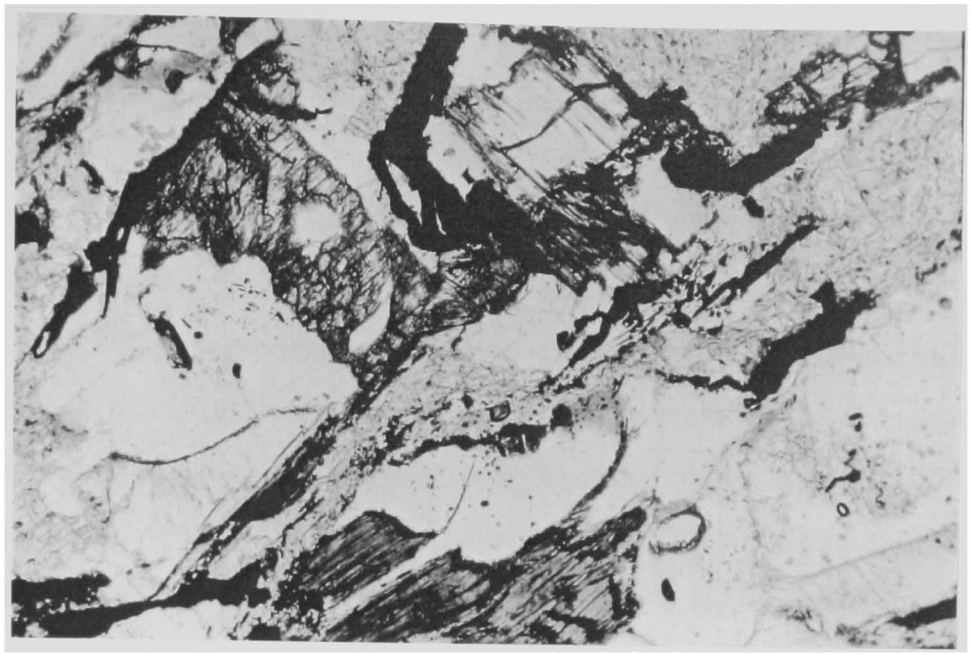

D.

Figure 10 (cont'd). *Mineral assemblages and textures within the Pilot Gneiss.* **C.** Graphitic schist: tremolite, graphite, muscovite, and biotite in matrix of plagioclase and quartz. Field of view is 1.3 mm in long dimension, plane-polarized light. Specimen FF-92. **D.** Garnetiferous tectonite: augen-like domains of garnet and quartz occur in matrix of quartz, chlorite, altered plagioclase, ± garnet and magnetite. Field of view is 7.0 cm in long dimension, shot in non-polarized light. Specimen from site 3 on Plate 1. Both sections perpendicular to local foliation, see Appendix 1A for exact sample localities.

The graphite is abundant along foliation planes and exhibits a conspicuous down-dip lineation which is parallel to that observed throughout the fault zone.

2.2.5 Mafic dikes/sills

Mafic intrusions are widespread within the Pilot Gneiss (Lewis 1975, Truman 1976, Kaygi 1979). Those observed in this study exhibit a wide variety of composition and texture, including coarse-grained, hornblende-rich bodies as well as finer-grained basaltic dikes or sills. In some cases, hornblende constitutes approximately 50-75% of the rock, although more often the units are composed of variable amounts of chlorite, actinolite, and epidote, together with calcite, quartz, and feldspar, with subordinate amounts of hornblende. It should be emphasized that these members of the Pilot Gneiss are extremely variable in their composition and may, in fact, represent a derivative of the amphibolitic layered gneiss, or *vice versa*. Where contacts are exposed, they are not obviously discordant to the predominant foliation, although any primary discordance may have been transposed during subsequent deformation. The timing of intrusion is uncertain, although the relations among similar units within the Brush Creek antilcinorium have been interpreted as either pre- or syntectonic (Kaygi 1979).

2.2.6 Garnetiferous tectonite

The only known occurrence of garnet within the Pilot Gneiss was discovered in a thin mafic layer within the layered gneiss complex (site 3 on Plate 1, also Appendix 1A). The garnet occurs in anhedral, augen-like domains, together with quartz, within a mylonitic matrix of quartz, chlorite, magnetite, and altered plagioclase (Figure 10D). Quartz within the augen exhibits undulatory extinction and only minor recrystallization as compared to quartz in the matrix. This association is thought to indicate that the garnet-

quartz domains were formed prior to mylonitization, during which much of the resulting shear strain was partitioned into the surrounding matrix.

Exposure of this unit is limited but nonetheless significant in that it may be the only record of an earlier, garnet-grade metamorphic event within the Pilot Gneiss. Interpretation of this assemblage will be treated further in the discussion section.

2.2.7 Leucocratic intrusions

Discontinous intrusions composed of quartz and perthite are another noteworthy constituent of the Pilot Gneiss (*e.g.* site 4 on Plate 1, also Appendix 1A). The intrusions are oriented parallel to the dominant foliation and often exhibit a pinch and swell morphology, although they do not themselves possess a discernible foliation; instead, the coarse-grained igneous texture is well-preserved. However, deformation is apparent in that the feldspar has been fractured and healed with quartz and much of the quartz exhibits undulose extinction, indicating that intrusion preceded the latest phase of low-temperature deformation. In addition to this coarse-grained phase, there are other finer-grained leucocratic intrusions throughout the Pilot Gneiss that exhibit similar late-stage fabrics, although complete characterization of these is beyond the scope of this study.

2.3 Ashe Formation

Along the southern margin of the area mapped in this study, the Little River Gneiss is overlain by clastic metasediments of the Late Proterozoic Ashe Formation (Rankin *et al.* 1973). The Ashe Formation comprises a wide variety of rock types including phyllite, metagreywacke, and metaconglomerate, although stratigraphic relationships among these units have not been established. Poor exposure of these units throughout the area has also obscured the location and characterization of the Ashe-

basement contact. However, recent work by Mies (1988) in northwestern North Carolina has led to the recognition of thrust-related mylonites along a similar basement-cover contact, suggesting that the Ashe-basement contact mapped in this study may, in fact, be a tectonic contact. Further characterization of the Ashe Formation is beyond the scope of this investigation.

2.4 Chilhowee Group metasediments

Within the study area, the Chilhowee Group is represented by a series of clastic metasediments located between the Fries fault and the Blue Ridge thrust (Figure 2). It is characterized by a wide variety of units including micaceous sandstone (Figure 11A), fine-grained quartz schist, phyllite, quartzite, and metaconglomerate. Many of the sandy units appear to have originated as feldspathic wackes and, less frequently, as quartz arenites containing accessory amounts of zircon and tourmaline. In contrast, the conglomeratic units often contain a distinct lithic component including clasts of polycrystalline quartz, quartzo-feldspathic material, and mudstone or phyllite. Regardless of grain size, however, the matrix mineralogy is typically characterized by the presence of muscovite, chlorite, and calcite aligned subparallel to the mylonitic foliation. Calcareous breccia composed of mudstone and siltstone clasts, quartz grains, and recrystallized oolites(?) was observed at one locality near Copper Valley (site 5 on Plate 1, also Appendix 1A). The stratigraphic position of this unit within the Chilhowee Group is uncertain, although the abundance of carbonate may indicate that it represents strata which are transitional into the overlying Shady dolomite.

Tectonic fabrics within the Chilhowee Group strata are highly variable and are partitioned according to both lithology and structural position within the fault zone. Asymmetric shear bands, similar to the "extensional crenulation cleavage" described by

Platt & Vissers (1980), are well developed within the fine-grained micaceous units adjacent to the overthrust block and indicate an up-dip (thrust-related) sense of shear (Figure 11B). The more competent quartz-rich units, on the other hand, lack the composite mesoscopic fabrics observed within the micaceous units, although strain within the quartzites is evident in the development of both crystallographic and shape-perferred orientation of relict detrital grains. A more detailed description of these features and their kinematic significance will be given in the following section.

A.

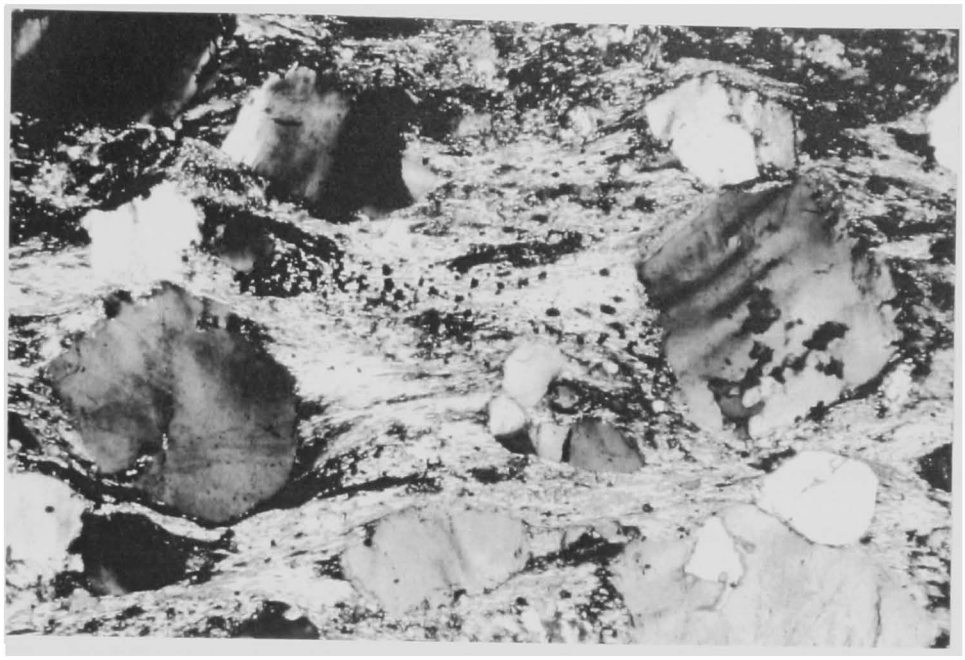

B.

Figure 11. *Characteristic mineralogy and texture of Chilhowee Group metasediments.* **A.** Foliation within micaceous quartz sandstone defined by new growth of white mica (along with chlorite, calcite, and magnetite) within the pressure shadows of detrital quartz grains. Field of view 3.25 mm in long dimension, cross-polarized light. Specimen CH-P1. **B.** Penetrative shear fabric in metasiltstone. Field of view is 6.5 mm in long dimension, plane-polarized light. Specimen FF-90. Both sections oriented perpendicular to the local foliation and parallel to lineation, see Appendix 1 for exact sample localities.

CHAPTER THREE:

KINEMATIC FRAMEWORK

Several methods of structural analysis were employed in this study in order to establish the three-dimensional kinematic framework within this portion of the Fries fault zone. The observations documented here include numerous asymmetrical structures—folds, oblique planar fabrics, and various porphyroclast systems—which generally support the contractional, northwest-vergent nature of the fault zone. This is further substantiated using crystallographic fabric analysis of quartz-rich tectonites within the fault zone. Tectonites from each of the three major units (Little River Gneiss, Pilot Gneiss, and Chilhowee Group) were analyzed, and the structural orientation of each specimen consistently approximates the best-fit, southeast-dipping foliation within the fault zone (see Figure 7B). In addition to the information gained concerning shear-sense within the fault zone, these analyses have elucidated significant variations in finite strain symmetry along the fault zone, which are correlated further with statistical analyses of deformed detrital grains within the Chilhowee Group.

3.1 Analytical techniques

The kinematic framework is defined on the basis of the inferred geometrical relationship between the predominant structural elements and the finite strain ellipsoid, whose principal axes—*X*, *Y*, and *Z*—define the orthogonal reference frame used in the following discussion. In this case, the direction of finite elongation (*X*) is represented by the southeast-plunging lineation (Figure 7B), while the direction of finite shortening (*Z*) is considered to be perpendicular to the mylonitic foliation. Therefore, in order to

evaluate the sense of shear within the fault zone (that is, whether the elongation lineation is the result of extension or contraction), oriented samples were cut perpendicular to the mylonitic foliation and parallel to lineation. The resulting plane of view, perpendicular to *Y*, thus contains both the minimum and maximum principal axes of the finite strain ellipsoid and is referred to as the "*XZ* section" in the following text and figures. All *XZ*-section figures and photomicrographs are presented as viewed toward the northeast, perpendicular to the local thrust transport direction.

Shear-sense determinations were made primarily on the basis of microstructures and petrofabrics observed in the *XZ* section of oriented slabs and thin sections, as well as by examining the larger, mesoscopic structures observed in field exposures. These observations were then supplemented by analysis of quartz *c*-axis preferred orientations within a variety of quartz-rich tectonites, including dynamically-recrystallized quartz veins as well as ductilely-deformed quartzites. Crystallographic orientations were measured in standard thin sections with the aid of a Leitz optical microscope equipped with a 3-axis universal stage and then converted from universal-stage coordinates to lower-hemisphere, stereographic coordinates through a FORTRAN program developed at Virginia Tech (R.D. Law, personal communication 1991). These data were then contoured on equal-area stereographic projections using the software package STEREOPLOT developed by Mancktelow (1989). As presented, all fabric diagrams are viewed toward the northeast within the *XZ* plane of the finite strain ellipsoid (see Figure 18, inset).

Quartz petrofabrics were also studied in conjunction with statistical ($R_f/\emptyset$) analyses of detrital grain shapes in order to quantify the three-dimensional strain symmetry within the fault zone. In conducting the $R_f/\emptyset$ analyses, the orientations and finite axial ratios of detrital quartz grains were measured in each of the three principal

sections (*XZ*, *YZ*, and *XY*) from several samples of Chilhowee Group metasediments. The data were then analyzed according to the $R_f/\emptyset$ method of Dunnet & Siddans (1971) using the software package MACSTRAIN developed by Kanagawa (1990). The resulting estimates of finite strain symmetry were then incorporated in a comparison of natural ***c***-axis fabrics with those produced in both experimental and computer simulation studies involving strict variations in the kinematic framework (*e.g.* Tullis *et al.* 1973, Tullis 1977, Dell'Angelo & Tullis 1989; and Etchecopar 1977, Lister & Hobbs 1980, Etchecopar & Vasseur 1987, Jessell & Lister 1990, respectively).

3.2 Asymmetric fold structures

Previous workers have recognized several northwest-vergent, kilometer-scale folds within the Chilhowee Group strata including: the structurally-paired Macks Mountain anticline and Copper Valley syncline of McDowell (1968), the Pilot Mountain anticline of Dietrich (1954), and the Brush Creek anticlinorium of Lewis (1975). These are complemented by both mesoscopic and micro-scale, asymmetric folds within the Chilhowee Group as well as folds observed within the Little River Gneiss and Pilot Gneiss (Lewis 1975, Truman 1976, and Kaygi 1979). However, the smaller-scale folds actually deform the mylonitic fabric and probably represent a subsequent deformation (Kaygi 1979). Alternatively, they may represent a single stage within a progressive northwest-vergent deformation, or even the manifestation of the same event under different rheological conditions (Lister & Williams 1983). Regardless of their timing, it is evident that asymmetric folds within the Fries fault zone record northwest-vergent, contractional deformation.

3.3 Rotation of planar fabrics

The classical models for fabric development in ductile shear zones (*e.g.* Ramsay & Graham 1970, Berthé *et al.* 1979a, 1979b, Ramsay 1980, White *et al.* 1980) illustrate how the sense of rotation associated with the transposition of an existing structural anisotropy may be utilized to determine the sense of shear within the zone. The tectonites examined in this study commonly exhibit composite planar fabrics similar to those described in the geological literature as composing "*S-C* mylonites" (see review in Hanmer & Passchier 1991). However, whereas the geometrical relationship between these planes, irrespective of their origin, may be used to determine the local shear direction, the recognition and genetic classification of these fabrics as *S* and *C* versus *C* and *C'* (described below) imposes significant constraints on the interpreted orientation and kinematic framework of the shear zone in question.

The mylonitic fabrics within this portion of the FFZ are composed of two distinguishable planar elements: a predominant mylonitic foliation, and a set of discontinuous, penetrative shear surfaces which offset the dominant foliation (Figure 12). Similar fabrics were first described (in a geologic context) by Berthé *et al.* (1979a, 1979b) and were referred to as *CS-C'* fabrics (figure 7 of Berthé *et al.* 1979b). Such fabrics are thought to develop at progressively higher shear strains, where the primary schistosity (*S*) is rotated into parallelism with, and offset along, discrete shear surfaces (*C*) oriented parallel to the shear zone boundaries (Figures 13A and B), ultimately transposing *S* into *C*. Continued attenuation of this composite *CS* (or *C*) fabric may then result in the development of secondary shear surfaces—more commonly referred to as "shear bands" (*C'* of Berthé *et al.* 1979b)—which, although oblique to the shear zone boundaries, indicate the same sense of rotation/transposition as that associated with the development of the predominant *CS* fabric (Figure 13C). By comparison, the mylonitic

A.

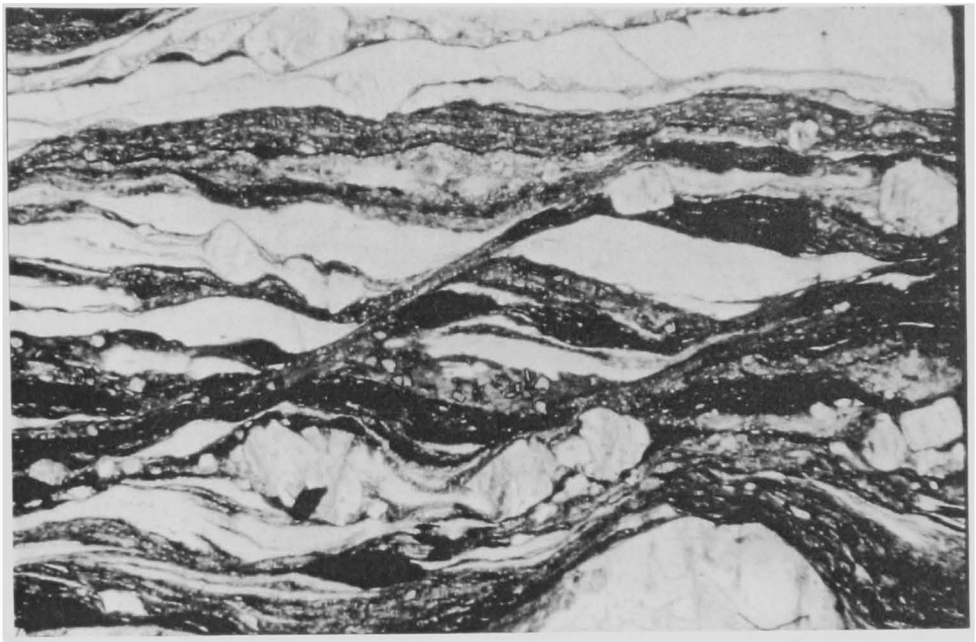

B.

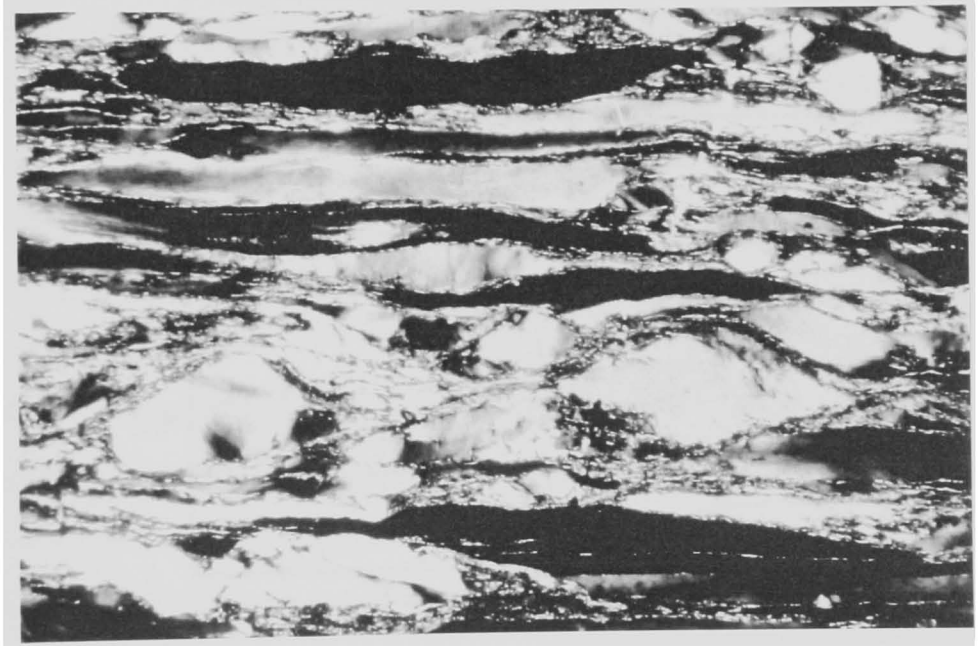

Figure 12. *Examples of asymmetric extensional shear bands.* **A.** Shear band offsetting quartz ribbons in Little River Gneiss ultramylonite. Specimen FF-P4. **B.** Shear-band offset of relict dertrital grain in Chilhowee Group quartzite. Specimen FF-62-1. Field of view in both is 6.5 mm in the long dimension, shot in cross-polarized light. See Appendix 1A for exact sample localities.

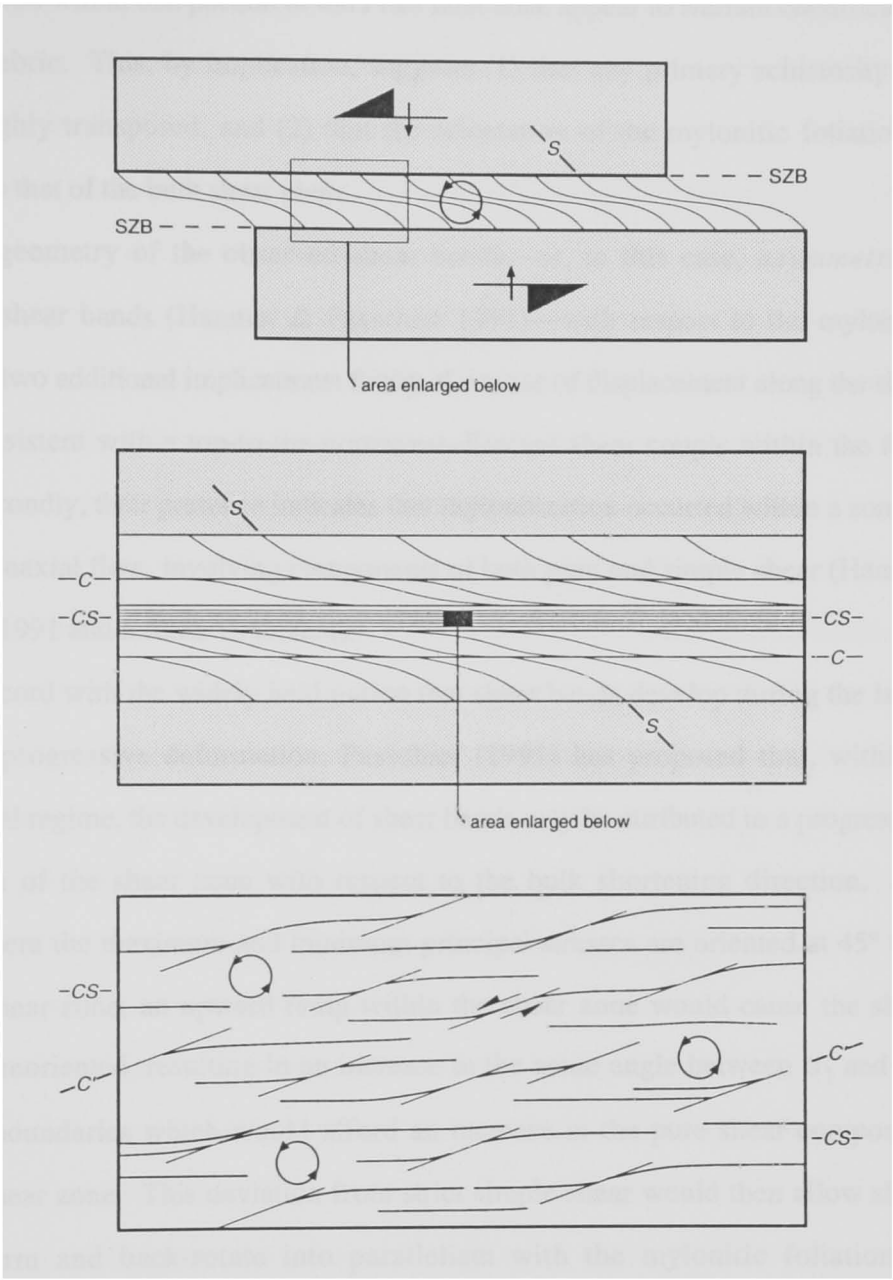

Figure 13. *Planar fabric elements of general noncoaxial flow.* SZB = shear zone boundary. **A.** First-order schistosity (*S*) and counter-clockwise vorticity expected within the shear zone. **B.** Transposition of primary schistosity along shear cleavage (*C*) oriented parallel to the shear zone boundaries. **C.** Orientation of asymmetrical extensional shear bands (*C'*) expected within the shear zone illustrated in **A**. According to Passchier (1991), these *C'* surfaces are the result of extension oriented parallel to the shear-zone boundaries. See text for discussion.

fabrics observed within this portion of the Fries fault zone appear to warrant classification as a *CS-C'* fabric. This, by implication, suggests (1) that any primary schistosity has been thoroughly transposed, and (2) that the orientation of the mylonitic foliation is subparallel to that of the bulk shear plane.

The geometry of the observed shear bands—or, in this case, *asymmetrical extensional* shear bands (Hanmer & Passchier 1991)—with respect to the mylonitic foliation has two additional implications: firstly, the sense of displacement along the shear bands is consistent with a top-to-the-northwest-directed shear couple within the fault zone; and secondly, their presence indicates that mylonitization occurred within a zone of general noncoaxial flow, involving components of both pure and simple shear (Hanmer & Passchier 1991 and references therein).

In accord with the widely held notion that shear bands develop during the latter stages of a progressive deformation, Passchier (1991) has proposed that, within a compressional regime, the development of shear bands may be attributed to a progressive reorientation of the shear zone with respect to the bulk shortening direction. For example, where the maximum and minimum principal stresses are oriented at 45° to a horizontal shear zone, an upward ramp within the shear zone would cause the shear fabric to be reoriented, resulting in an increase in the acute angle between σ_1 and the shear zone boundaries which would afford an increase in the pure shear component within the shear zone. This deviation from strict simple shear would then allow shear bands to form and back-rotate into parallelism with the mylonitic foliation as displacements along shear bands are accomodated by extension of the shear zone and its wall rock (Figure 13C). Progressive back-rotation of shear bands has also been suggested by other workers (*e.g.* Berthé *et al.* 1979b, Platt & Vissers 1980) who have documented a consistent decrease in the angle between shear bands and foliation

corresponding to an apparent increase in the amount of finite strain. Similarly, in this study, there is a marked decrease in the acute angle between the mylonitic foliation and offsetting shear bands (*CS–C'*) with increasing proximity to the Little River Gneiss/Pilot Gneiss contact (Figure 14) where the intensity of grain-size reduction and fabric development suggests that finite strain is greatest.

These spatial relationships suggest that there is a fundamental relationship between finite strain and shear band geometry. However, the starting orientation of the shear bands may have been influenced by the rheological characteristics of their host, which may vary according to its microstructural characteristics as well as the orientation of the mylonitic foliation within the prevailing stress field (Platt & Vissers 1980). Alternatively, if the shear bands are assumed to have had similar starting orientations with respect to the mylonitic foliation, then the finite variability in these shear band geometries may be due to heterogeneous shear strain within the fault zone; that is, a progressive decrease in the acute angle would imply a progressive increase in the magnitude of finite strain due to pure shear. In either case, however, the composition of these mylonitic fabrics necessitates a significant (although relatively minor) component of extension, resulting from pure shear, oriented parallel to lineation within the plane of foliation. Deformation of this sort may have been accommodated solely by extension of the shear zone toward the northwest, in the direction of thrust transport. These observations are in accord with the interpreted kinematic framework of general noncoaxial flow, which is possibly the result of progressive imbricate stacking (*cf.* figure 9c in Passchier 1991) farther to the southeast within the Blue Ridge thrust complex.

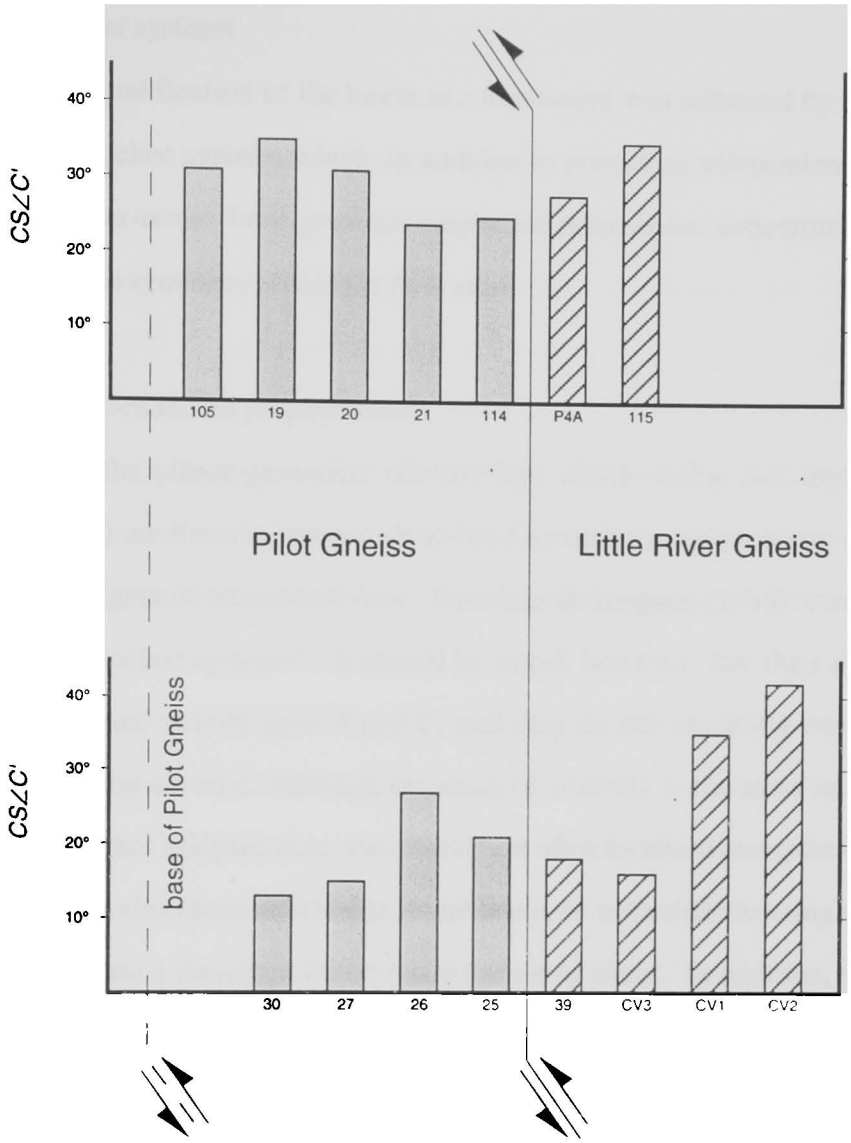

Figure 14. *Geometric relationship between predominant mylonitic foliation (CS as in Figure 13) and shear bands (C') with respect to unit boundaries.* Both transects in the vicinity of Copper Valley. Spacing of sites is not to scale. The progressive decrease in the acute angle may be interpreted to reflect an increase in the magnitude of finite strain due to pure shear. CG, LRG, PG same as in Figure 2.

3.4 Porphyroclast systems

Further qualification of the kinematic framework was achieved by the study of various porphyroclast systems which, in addition to providing independent criteria for determining shear-sense, have provided important information concerning the three-dimensional strain symmetry within the fault zone.

3.4.1 Shear band-modified porphyroclasts

Beyond the planar-geometric relationships which define *S-C* mylonites (see previous section) are the conspicuous shear band-modified porphyroclasts which often form in zones of general noncoaxial flow. Passchier & Simpson (1986) refer to these as "s_b-*type* porphyroclast systems". It should be noted, however, that their definition of this "type" is based strictly upon *S* and *C*, and they do not explicitly consider those systems defined by *C* and *C'* although the sense of vorticity is the same in either case. Within the mylonites analyzed here, shear bands are often localized along the boundary of relatively rigid grains (such as feldspar, hornblende, or actinolite) forming asymmetric tails which indicate a dominant thrust-related sense of shear. In addition, very few of these porphyroclasts exhibit subordinate shear bands which indicate the opposite sense of shear. These subordinate sets are consistent with top-down-to-the-southeast (extensional) deformation, although they appear to have formed during the same metamorphic event as the thrust-related fabrics and, therefore, are considered to reflect the deviation toward general noncoaxial flow within the fault zone.

3.4.2 Pressure fringe geometry

Pressure fringes are another microstructural element which have facilitated an assessment of the bulk deformational path, as well as the three-dimensional symmetry of

finite strain within the fault zone. The porphyroclast system analyzed here occurs within a chloritic metasandstone member of the Chilhowee Group (FF80 on Figure 18, see Appendix 1B for exact sample locality) and is composed of euhedral magnetite porphyroblasts which are flanked by pressure fringes of quartz (Figure 15). However, both the geometry and length of the pressure fringes vary among the three principal sections with respect to the imposed kinematic framework. In the *XZ* section (Figure 15A), each magnetite crystal is associated with four sets of fibrous quartz overgrowths which display a trajectory of parallel curves between the crystal and the matrix, two of which intersect the face of the crystal at 90°. In general, the distribution of quartz fibers within this section indicates extension in the *X* direction. The *YZ* section, on the other hand, shows a negligible amount of extension in either the *Y* or *Z* direction (Figure 15B), although the presence of minute quartz fibers along the face oriented perpendicular to *Y* indicates that there has been minimal extension in the *Y* direction. In accord with these observations, the distribution of fibers within the *XY* section also indicates that deformation was accommodated primarily by extension in the *X* direction. All together, these relations define the three-dimensional symmetry of finite strain as approximately plane strain (*cf.* figures 8 and 9 in Law & Potts 1987).

The internal geometry of pressure fringes observed within the *XZ* section are remarkably similar to some of the pressure shadow geometries modelled by Etchecopar & Malavieille (1987). According to their computer simulations—which utilize variations in the amount of pure shear versus simple shear and magnitude of shear strain—the geometry of the fibers in the *XZ* section of specimen FF80 (Figure 15A, this study) is consistent with having developed in a kinematic framework of noncoaxial plane strain (*cf.* figure 11b in Etchecopar & Malavieille 1987). It should also be noted that the asymmetry of the fibers displayed in Figure 15A is consistent with a thrust-related (or

A.

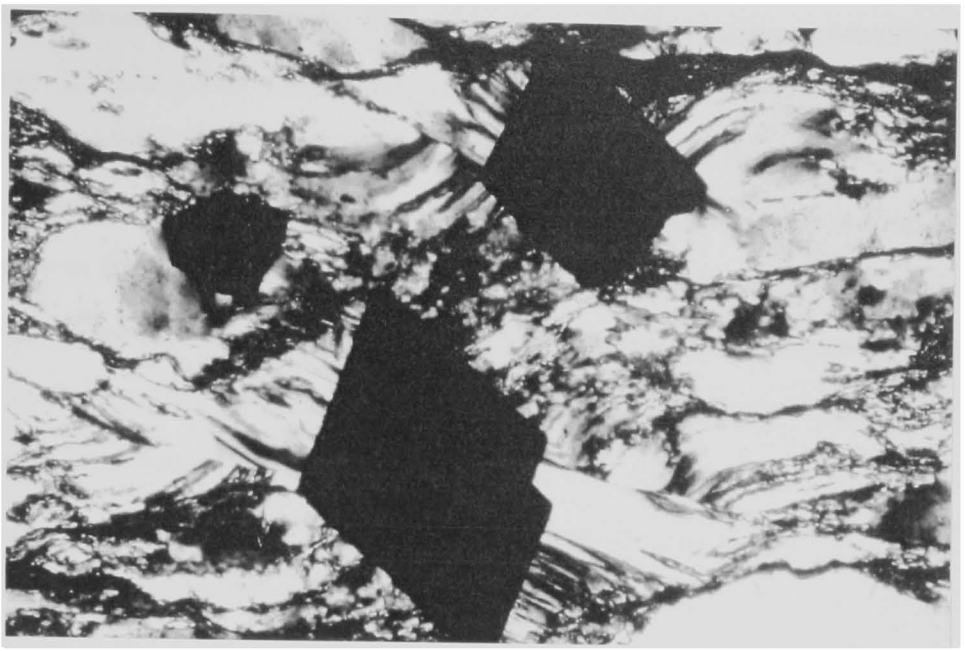

B.

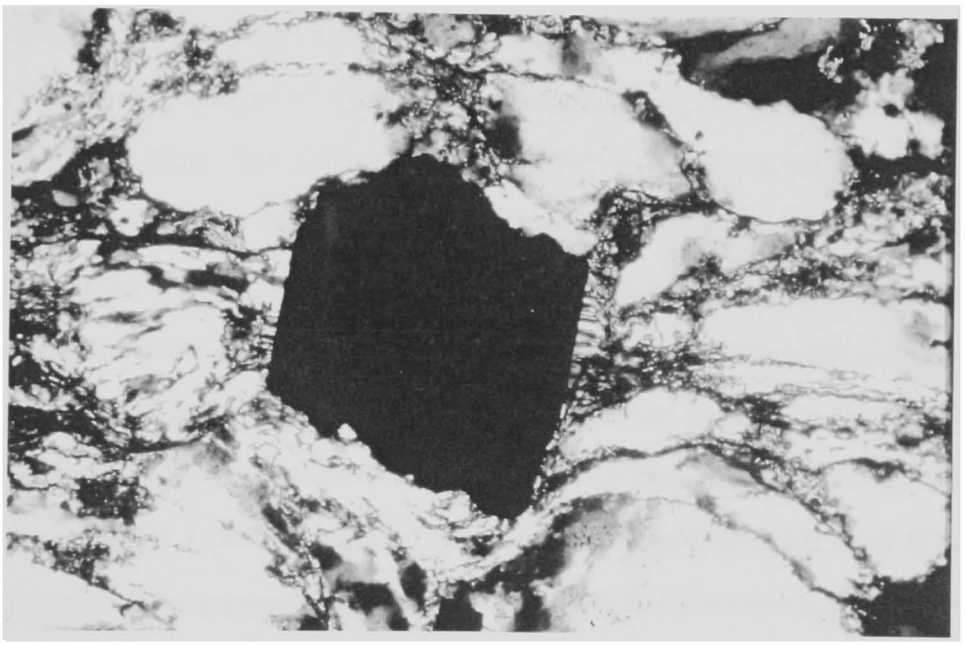

Figure 15. *Pressure fringe geometries associated with magnetite porphyroclasts.* **A.** Complex pressure fringe geometries observed within the *XZ* section indicates that deformation was strongly noncoaxial. **B.** *YZ* section of same specimen showing only limited development of pressure fringes within the plane of foliation (horizontal) adjacent to porphyroclast. Field of view is 6.5 mm in the long dimension, shot in cross-polarized light. Specimen FF80. See text for discussion, Appendix 1B for exact sample locality.

top-to-the-northwest) shear couple. This comparison also places some constraint on the magnitude of shear strain within the fault zone. Whereas the fibers simulated by Etchecopar & Malavieille (1987) for a γ=5 extend farther than those in the specimen described here, it is reasonable to assume that the shear strain within this portion of the fault zone was less than γ=5. Any further discrepancies between these simulated and natural fabrics may, of course, be attributed to the strictness of their model parameters throughout the simulated deformational history *versus* those which actually governed the formation of these natural pressure fringes.

3.4.3 Quartz ribbon porphyroclasts

A top-to-the-northwest sense of shear is also evident in the development of monomineralic quartz porphyroclasts. The porphyroclast system analyzed here is hosted within a dynamically recrystallized quartz vein situated along the approximate contact between the Little River Gneiss and Pilot Gneiss (FF72 on figure 18, see Appendix 1A for exact sample locality). The specimen consists primarily of elongate, newly formed grains that exhibit a strong shape-preferred orientation which is oblique to the main foliation (Figure 16A), whereas the older grains tend to exist as ribbon-like domains of undulose extinction and incipient recrystallization oriented parallel to the foliation. Further discussion of this oblique grain-shape fabric and its kinematic significance will be held until section 3.5.1: Shape-preferred orientation. The porphyroclast itself (Figure 16B) is interpreted as representing a portion of an originally monocrystalline quartz ribbon which, during strongly noncoaxial flow, has undergone progressive rotation with respect to the adjoining portions of the ribbon which now form the porphyroclast tails. This scenario is similar to the model proposed by Lister & Williams (1983) for the generation of "fold packets" during progressive simple shear. Their model suggests that

flow perturbations within a structurally anisotropic medium may become amplified, leading to rotation of the layers as the bulk, shear-induced vorticity is locally converted to spin. Although it is difficult to substantiate the existence of a structural anisotropy within this pure quartz mylonite, it is speculated that there was sufficient contrast in the competancy of the ribbon versus its matrix which allowed any perturbations (such as thickness variations) to be amplified (*cf.* figure 6 in Lister & Williams 1983). The inferred spin of the porphyroclast with respect to its tails is supported by discriminate analysis of quartz ***c***-axis orientations within the various components of the porphyroclast system (Figure 17). Figure 17A illustrates how the system was broken up into five sectors including: the porphyroclast itself, the two tails, and the two adjacent areas composed of dynamically recrystallized quartz. Each of the locations at which a crystallographic orientation was measured are marked by symbols corresponding to one of the three sector classifications. The ***c***-axis orientations within each sector were then plotted as individual stereographic projections for comparison (Figure 17B). A composite plot of these orientations (Figure 17C) clearly illustrates an apparent counter-clockwise rotation of ***c***-axes within the porphyroclast with respect to those in the porphyroclast tails, although this does assume that the lattice orientations were uniform to begin with. Such an assumption does, in fact, appear to be justified on the basis of the optical continuity within other ribbons in the sample which have not been deformed in the same manner. Furthermore, the apparent rotation of these axes within this porphyroclast system is consistent with both the expected spin direction for Lister & Williams' (1983) model and the sense of vorticity expected within this thrust-related shear zone (as illustrated in Figure 13C).

A.

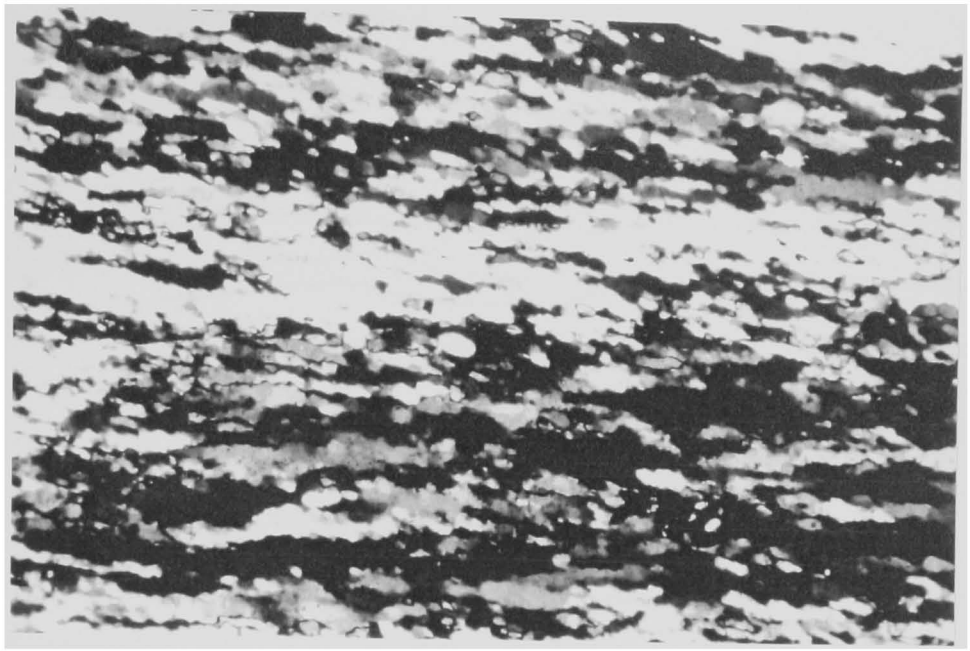

B.

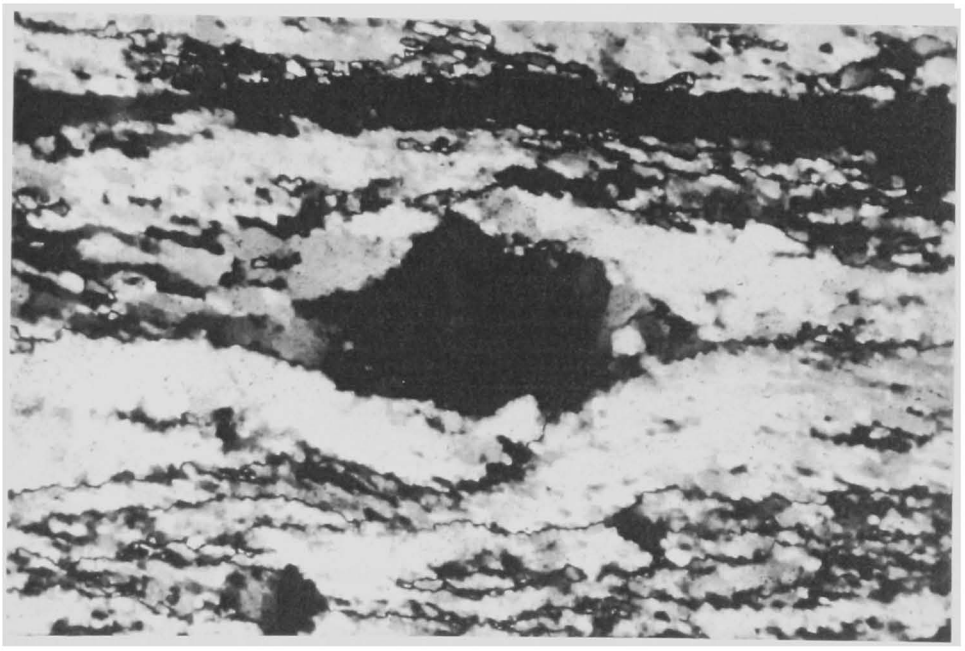

Figure 16. *Porphyroclast and matrix characteristics in quartz mylonite.* **A.** Oblique grain-shape fabric of recrystallized grains forming the matrix of a mylonitized quartz vein. *XZ* section, specimen FF72. **B.** Quartz porphyroclast hosted within the dynamically recrystallized matrix shown in **A.** Discriminant crystallographic analysis of this porphyroclast system suggests that it was developed during sinistral (thrust-related) shear (see Figure 17). Field of view is 1.3 mm in the long dimension, shot in cross-polarized light. See text for discussion, Appendix 1A for exact sample locality.

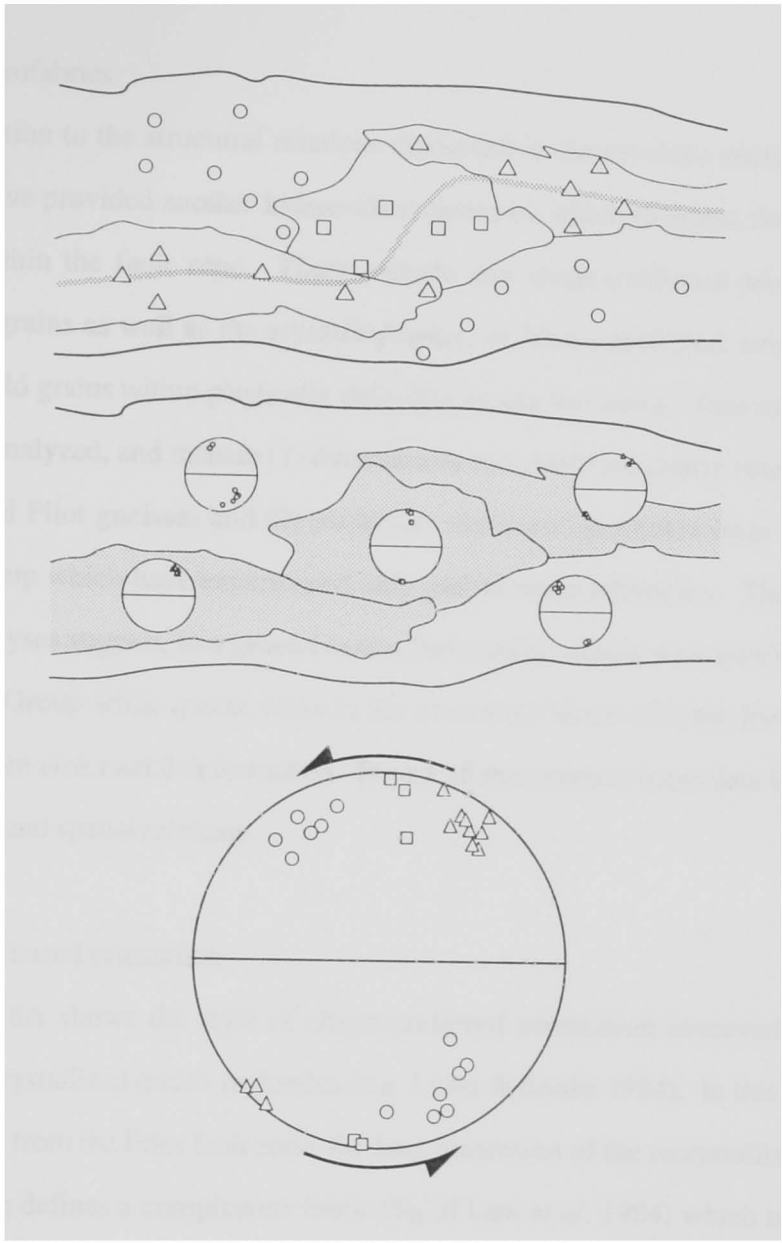

Figure 17. *Progressive reorientation of quartz* ***c****-axes in a rotating pophyroclast.* **A.** Line drawing of porphyroclast system shown in Figure 16B. Stippled line represents the interpreted medial surface of the deformed quartz ribbon. Geometric symbols represent points where ***c***-axis orientations were measured and are keyed to specific structural domains: triangles, relatively undeformed porphyroclast tails; squares, rotated porphyroclast; circles, recrystallized matrix. **B.** Lower hemisphere projections of ***c***-axis orientations within each domain. **C.** Composite view of ***c***-axis orientations illustrating the counter-clockwise sense of vorticity within this porphyroclast system. Diagrams are oriented as *XZ* sections: perpendicular to the local foliation and parallel to lineation, viewed toward the northeast. See text for discussion.

3.5 Quartz petrofabrics

In addition to the structural relations discussed in the previous sections, quartz petrofabrics have provided another independent means by which to assess the kinematic framework within the fault zone. These include any shape-preferred orientation of recrystallized grains as well as the crystallographic, or lattice-preferred, orientation of both new and old grains within plastically deformed quartz tectonites. Two categories of samples were analyzed, and include (1) dynamically recrystallized quartz veins from the Little River and Pilot gneisses and (2) plastically deformed quartzites from within the Chilhowee Group which have experienced only partial recrystallization. The resulting petrofabric analyses suggest, in a general sense, that coaxial strains were partitioned into the Chilhowee Group while quartz veins in the overthrust block of Little River Gneiss experienced more noncoaxial deformation. Figure 18 summarizes these data in terms of their geological and spatial relations.

3.5.1 Shape-preferred orientation

Figure 16A shows the style of shape-preferred orientation observed in many dynamically recrystallized quartz mylonites (*e.g.* Lister & Snoke 1984). In this example, as well as others from the Fries fault zone, the long dimension of the recrystallized grains in the *XZ* section defines a conspicuous fabric (S_B of Law *et al.* 1984) which is inclined more steeply to the southeast than the pervasive mylonitic foliation (S_A). It is important to note, however, that the long axis of these grains may not behave as material lines that might otherwise be used in determining the orientation of the finite strain ellipsoid. Instead, the elongation of these grains may reflect only one cycle of recrystallization (Means 1981) during which the deformed (elongate) grains experience an increase in dislocation density leading to the formation of new grains which are subject to

Figure 18. *Relative sample locations and c-axis fabric diagrams of specimens used in determining the three-dimensional kinematic framework within the Fries fault zone.*

Crystallographic fabric diagrams presented as lower-hemisphere projections, contoured at 1, 2, 5, 10, 15, 20, 25, and 30 times uniform distribution. S_A-S_B insets are referenced to the same coordinates as fabric diagrams. $Ø_{xx}$ symbolizes localities at which samples (subscript number) were collected for $R_f/Ø$ analyses. AF, CG, LRG, PG same as in Figure 2. See text for discussion, Appendix 1 for exact sample localities.

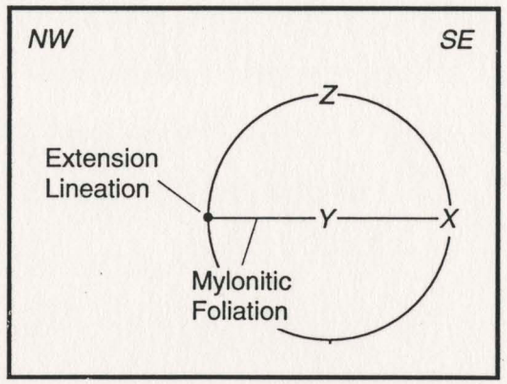
NW
SE
Z
Extension
Lineation
Y
X
Mylonitic
Foliation

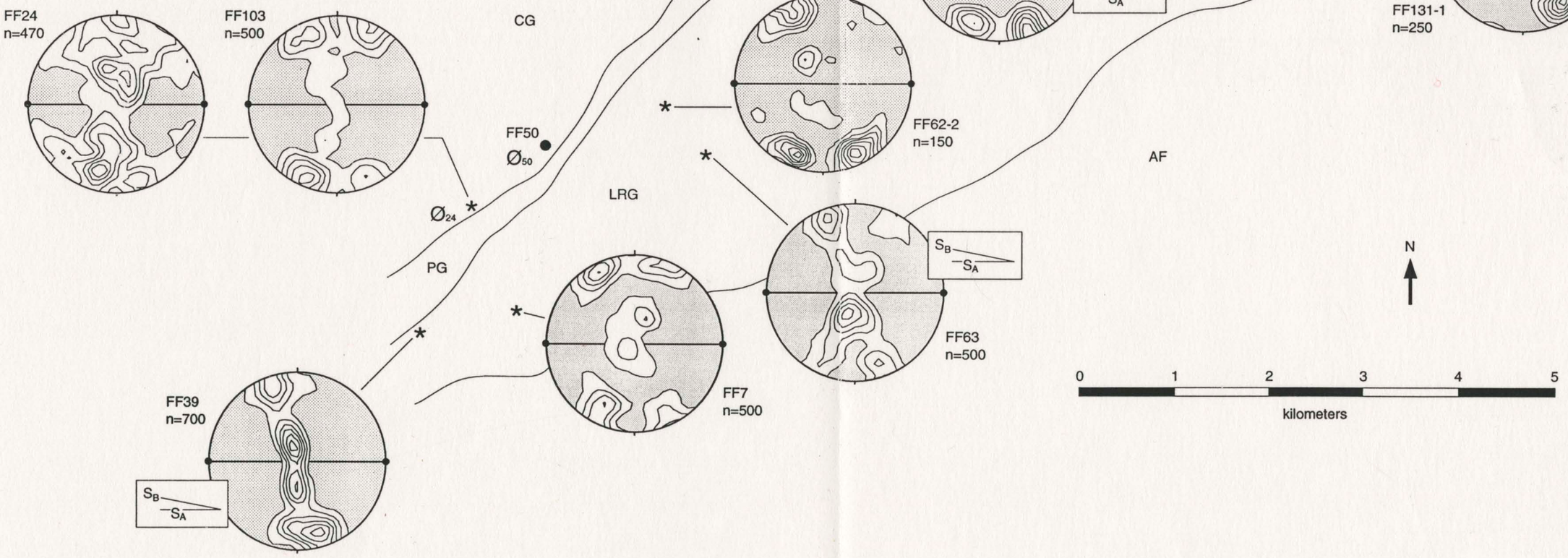
FF24
n=470
FF103
n=500
FF50
Ø50
Ø24
PG
CG
FF62-1
n=500
Ø62-1
PG
FF78
n=500
CG
PG
Ø78
FF80
FF72
n=350
SB
SA
LRG
FF131-1
n=250
FF62-2
n=150
AF
LRG
FF63
n=500
FF7
n=500
FF39
n=700
SB
SA
N
0
1
2
3
4
5
kilometers

subsequent cycles of deformation and recrystallization (see review of *strain insensitive fabrics* in Hanmer & Passchier 1991). Hanmer & Passchier (1991, p. 26) also point out that "the degree to which the foliation [S_B] reflects the instantaneous stretching axes, rather than the principal finite strains, is a function of the relative efficiency of the fabric-weakening processes" such as dynamic recrystallization. Therefore, regardless of how many cycles of recrystallization have occurred, the kinematic significance of this petrofabric lies in the fact that S_B must be oriented between the instantaneous and finite stretching axes of the shear zone, and therefore defines the extensional quadrants with respect to the mylonitic foliation (S_A). For example, in Figure 16A, the sense of obliquity between S_A and S_B indicates a sinistral (top-to-the-northwest) shear sense.

In addition to the fabric illustrated in Figure 16A, which was collected from the contact zone between the Little River and Pilot gneisses, similar examples of grain-shape preferred orientation were observed elsewhere within the Little River Gneiss (FF39 and FF63 on Figure 18). All of these occur within quartz veins which vary in width from 1 to 10 centimeters, where the angle between S_A and S_B is remarkably uniform (*ca.* 10°-12°) and the sense of obliquity consistently indicates top-to-the-northwest, thrust-related deformation.

3.5.2 Crystallographic-preferred orientation

Ten quartz tectonites were analyzed for ***c***-axis preferred orientation. Four of these represent quartz-rich metasedimentary horizons within the Chilhowee Group, while the remaining six consist of mylonitized quartz veins from within the Little River and Pilot gneisses (see corresponding locations on Figure 18 and Plate 1). These differences in protolith, as well as the natural variations in strain path, are reflected in the variety of microfabrics described in the following sections. In the broadest sense, these variations

in crystallographic fabric may be broken down into two categories: first, those fabrics defined by dynamically recrystallized grains, as observed in the recrystallized quartz veins; and, second, those fabrics that are defined solely upon the crystallographic orientation of relict detrital grains, as in the quartzites of the Chilhowee Group.

3.5.2.1 Recrystallized quartz veins

Petrofabric analysis of recrystallized quartz veins from within the Little River Gneiss has revealed strong crystallographic-preferred orientation of new grains. Grain sizes vary widely among the six samples, from 10 to 100 μm, although there does not appear to be any systematic variation in petrofabric with grain size. Grain shapes, however, are generally elongate and may be oriented with their long axes oblique to the mylonitic foliation, as is the case in samples FF39, FF63, and FF72 (see section 3.5.1). In contrast, the microstructure (*i.e.* grain shape and orientation) of sample FF62-2 is characterized by elongate grains oriented subparallel to the mylonitic foliation; this specimen is distinguished by its unusually high phyllosilicate content which undoubtedly facilitated grain-boundary sliding during deformation.

A common feature of these *c*-axis fabrics (excluding FF7 and FF131-1) is their asymmetric disposition with respect to the mylonitic foliation. In the case of specimen FF39, the ***c***-axes are distributed along a single girdle through Y, although the girdle is inclined with respect to the X and Z directions. According to Schmid & Casey (1986), such fabrics are the result of strongly rotational deformation (approximating simple shear), where the sense of shear corresponds to the direction in which the girdle is apparently rotated away from the Z direction: a counter-clockwise rotation in this example. In the following discussion, a counter-clockwise rotation of the ***c***-axis girdle will be considered *positive*, a clockwise rotation *negative*. Hence, the *positive* girdle of

specimen FF39 represents a top-to-the-northwest (thrust) displacement along the Little River Gneiss–Pilot Gneiss contact. A similar distribution of ***c***-axes is observed within specimen FF72, although the concentration of points within the *XZ* plane (periphery of the diagram) is considerably greater. Comparison of this contoured plot with Figure 17C suggests that the ***c***-axes oriented in a *positive* sense represent the dynamically-recrystallized matrix while the *negative* points correspond to older grains which have not thoroughly recrystallized. All together, the distribution of ***c***-axes within this specimen delineates a rather symmetric skeletal fabric (Lister & Williams 1979) which may be interpreted as the result of coaxial strain. However, given the previous discussion regarding the antiquity of the *negative* grains (section 3.4.3), it seems reasonable to disregard these points when interpreting the kinematic significance of the recrystallized fabric. The ***c***-axis petrofabric of specimen FF72 is therefore considered as a discontinuous single girdle representing noncoaxial (thrust-related) shear strain along the Little River Gneiss–Pilot Gneiss contact.

In contrast to the fabrics described above, the ***c***-axes of specimen FF63 define a more symmetric, crossed-girdle fabric (*Type II* of Lister 1977). Schmid & Casey (1986) suggested that the symmetric nature of such fabrics is indicative of coaxial deformation and that *Type II* fabrics, in particular, represent a departure from plane strain toward the constrictional field. While this may be the case, it is important to note that this specimen is composed of a discontinuous, or broken, crossed-girdle in which the *positive* girdle is more strongly developed, thus suggesting a noncoaxial strain component associated with top-to-the-northwest thrusting. This kinematic interpretation is supported by the obliquity between S_A and S_B in the same specimen. In view of the single-girdle fabrics found along the base of the Little River Gneiss, the coaxial component of specimen FF63 may simply reflect variations in the strain path with increasing proximity to the thrust

contact; that is, an increased component of simple shear toward the base of the Little River Gneiss (*cf.* Law *et al.* 1986, Law 1987). Alternatively, this fabric may be the result of overprinting coaxial and noncoaxial deformations, although this study has found no other evidence of such, or this broken fabric may be interpreted as the result of relatively low finite strain in strict simple shear (*e.g.* Schmid & Casey 1986, Jessell & Lister 1990). The apparent coaxial strain recorded in specimen FF7 represents that associated with the transposition of foliation from the protolith gneiss into the predominant mylonitic foliation of the Little River Gneiss. This may be used to infer that the early phases of deformation within the Little River Gneiss were coaxial (at least locally), whereas subsequent deformations evolved toward more noncoaxial strains. Such a conclusion is obviously premature, although it is in marked contrast to Kaygi's (1979) interpretation that flattening strains were more dominant during the later stages of deformation.

3.5.2.2 Deformed detrital grains

The quartzite members of the Chilhowee Group record a very different degree of dynamic recrystallization from that recorded within the quartz veins of the Little River Gneiss. In particular, the microstructure of the quartzites is distinguished by the presence of relict detrital quartz grains which have been variably stretched and flattened within the plane of foliation. Optical characteristics such as undulose extinction and deformation lamellae within the relict grains indicate that deformation was accommodated principally by intracrystalline slip and recovery (White 1973, Marjoribanks 1976, Bouchez 1977, Law 1986). Ultimately, however, these processes have resulted in the deformation of individual detrital grains into optically distinct lenses and ribbons (see Figure 12B) while producing a strong preferred orientation of quartz ***c***-axes in a given sample.

Discriminant petrofabric analysis of these detrital grains, excluding the recrystallized grains between adjacent ribbons and lenses, has revealed symmetric fabrics indicating coaxial deformation in each of the four specimens (FF24, FF103, FF62-1, and FF78 in Figure 18). This is evident in the symmetric disposition of their skeletal outlines with respect to both foliation and lineation (*cf.* Lister & Williams 1979, Lister & Hobbs 1980, Schmid & Casey 1986, Etchecopar & Vasseur 1987). However, the obvious variation among these fabrics suggests that there are significant differences in the symmetry of finite strain along the fault zone.

Specimens FF62-1 and FF78 are similar to the *Type I* (plane strain) fabrics described by Lister (1977), although the density of ***c***-axes oriented parallel to *Y* suggests that the kinematic framework may have deviated toward constrictional strain (Schmid & Casey 1986). The theoretical considerations of Lister & Hobbs (1980) are in general agreement with this and suggest that such tight concentrations approximating the *YZ* plane are developed within the constrictive field. In contrast, specimens FF24 and FF103 (from the same field site) are characterized by broader concentrations of ***c***-axes about the *Z* direction. Such small-circle distributions and point maxima (as in FF103) have been correlated with flattening strains in other studies (*e.g.* Marjoribanks 1976, Lister & Hobbs 1980, Price 1985, Law 1986), although the bridge of points through *Y* implies a component of plane strain (Schmid & Casey 1986). In fact, similar point-maxima fabrics have been produced under experimental conditions of plane strain (figure 2b in Tullis 1977). Furthermore, the presence of ***c***-axis maxima oriented between *Y* and *Z* (in FF24) is reminiscent of Lister's *Type I* fabric.

On the basis of these correlations, it is apparent that the quartzites within the footwall of the Fries fault zone record a variety of coaxial strain symmetries, including plane strain as well as flattening and constriction. However, further correlation of these

petrofabrics with their respective strain ellipsoids is needed in order to substantiate the inferred kinematic framework. Therefore, quantitative estimates of finite strain and strain symmetry are provided in the following section as an additional constraint on the kinematic framework depicted by these fabrics.

3.6 $R_f/\emptyset$ analyses—deformed detrital quartz grains

The apparent plasticity of relict detrital quartz grains provides a basis for assuming that their current three-dimensional shape may be used as strain markers for estimating the finite strain ellipsoid for any given sample. With this assumption, a statistical analysis of deformed detrital grains was conducted on four quartzite specimens as a quantitative measure of finite strain within the Chilhowee Group tectonites.

Following the $R_f/\emptyset$ method outlined by Dunnet (1969) and Dunnet & Siddans (1971), the orientations and axial ratios of deformed grains were measured in each of the three principal kinematic sections. Grains were not included in the sample population where recrystallization had obviously modified the aspect ratio, or in cases where the nature of a grain boundary was ambiguous. These data were then analyzed using the computer software package MACSTRAIN (Kanagawa 1990) in order to estimate the two-dimensional finite strain within each section. This method takes into account the initial ellipticities of detrital marker grains (Figures 19-22 and Table 1). The resulting strain ratios were then used to back-calculate each elliptical section of the corresponding ellipsoid (see row 2 in Table 1). In three of the four samples, the back-calculated values (Rs') were within 3% of the independently calculated strain values (Rs). These two-dimensional strain values were then used construct the finite strain ellipsoids for FF24, FF50, and FF78 (Figure 18, see Appendix 1 for exact sample localities). However, the back-calculated values for specimen FF62-1 are off by ~30 to 50 percent and may not be

used as a reliable indication of finite strain at the corresponding field site. This disparity may be attributed to the effects of late-stage pressure solution (evident in thin section) which could have effectively reduced the Z dimension and thus accentuated the apparent finite strain in both the XZ and YZ sections; although simple expansion of the Z dimension does not resolve the problem. Alternatively, these data may reflect errors in measurement. A simple comparison of the c-axis fabrics from samples FF62-1 and FF78 (Figure 18) suggests that both record similar finite strains. Thus, using the strain data of FF78 (Table 1) as a model, an internally-consistent ellipsoid was back-calculated for FF62-1 by simply decreasing its measured XY ratio from 4.30 (Table 1) to Rs = 3.00, yielding an error of ±3 percent. Internal consistency could also have been attained by increasing the measured XZ ratio to Rs = 11.00, although by manipulating the XY ratio instead, the symmetry of FF78 is maintained in accord with the petrofabric correlation.

The significance of these data in defining the kinematic framework will be discussed in the following section.

3.7 Correlation of $R_f/\emptyset$ analyses and quartz petrofabrics

The three-dimensional strain data reported in the previous section are summarized in Figure 23 with respect to the finite strain fields of Flinn (1962). In general, the combined results of this and previous studies (see Table 2) define a narrow range of flattening strains that trend toward plane strain, extending into the constrictional field with increasing strain magnitude (Figure 23A). The higher-magnitude strains appear to be localized within the central portions of the study area, while lower-magnitude flattening-field strains are found along strike to the east and west.

Comparison of the petrofabrics discussed in section 3.5.2.2 with these estimates of finite strain symmetry are in excellent agreement with the findings of Schmid & Casey (1986) as well as the theoretical models of Lister & Hobbs (1980). In particular, the correlation of modified *Type I* cross-girdle fabrics (*e.g.* FF62-1 and FF78) with conditions of plane strain deviating toward constriction is clearly supported by the data presented here (see Figure 23B). In addition, the petrofabrics attributed to flattening deformation (FF24 and FF103) are correlated closely with finite strain estimates that plot in the flattening field (FF24 and FF50).

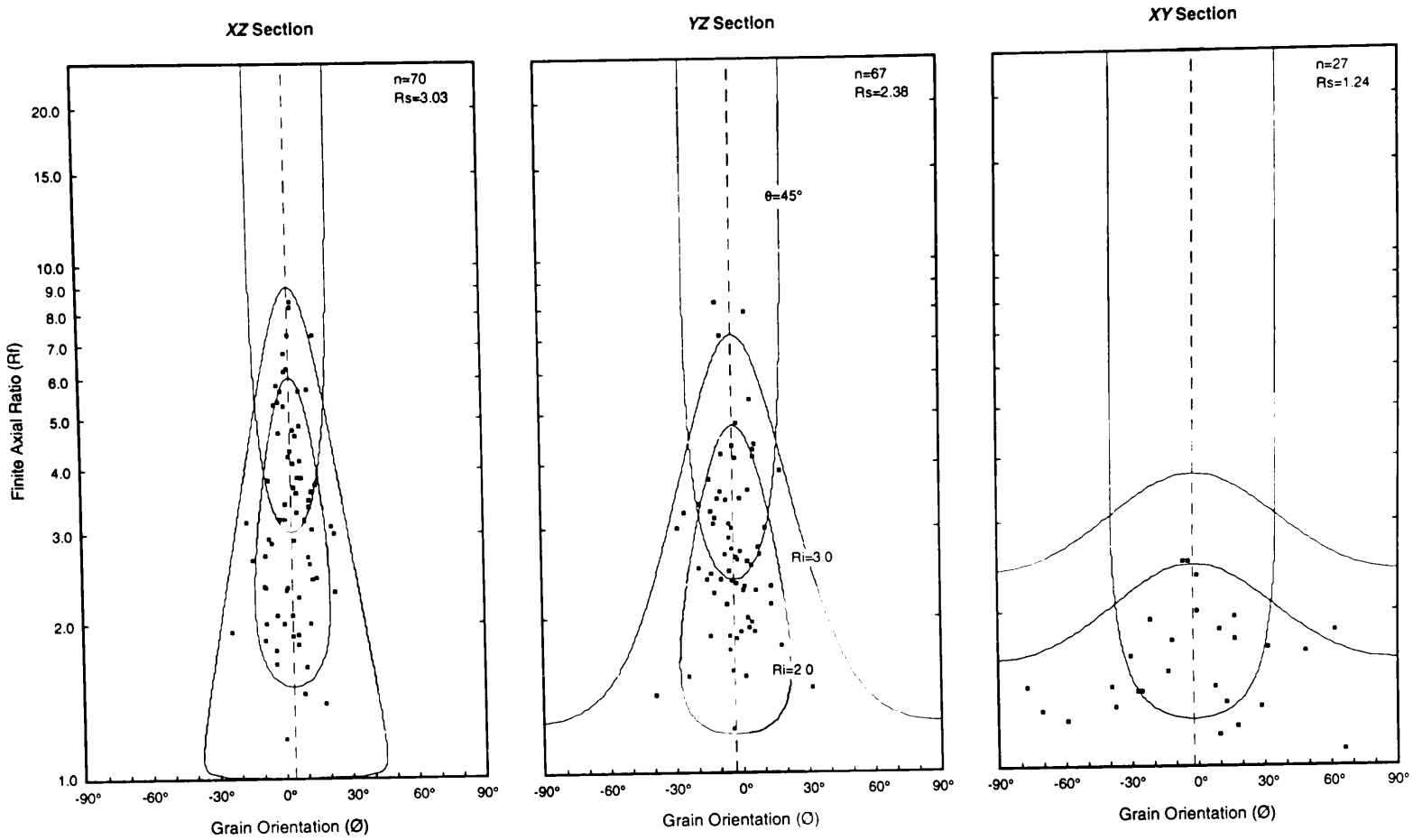

Figure 19. $R_f/\emptyset$ plots for the three principal sections of sample FF24. Calculated strain ratio (R_s) indicated in upper right corner of each. R_i and θ curves determined using MACSTRAIN (Kanagawa 1990). See text for discussion.

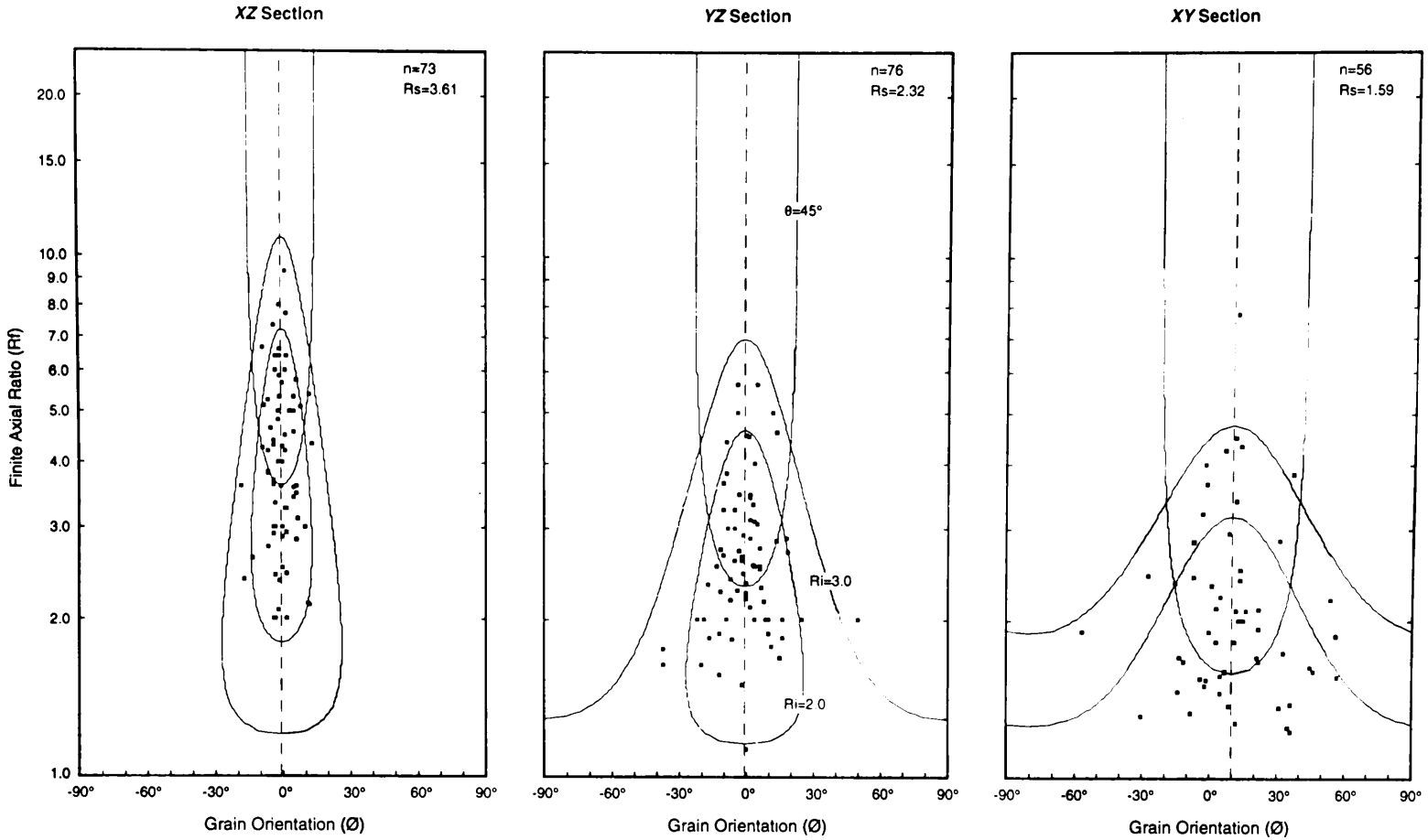

Figure 20. *Rf/Ø* plots for the three principal sections of sample FF50. Calculated strain ratio (R_s) indicated in upper right corner of each. R_i and θ curves determined using MACSTRAIN (Kanagawa 1990). See text for discussion.

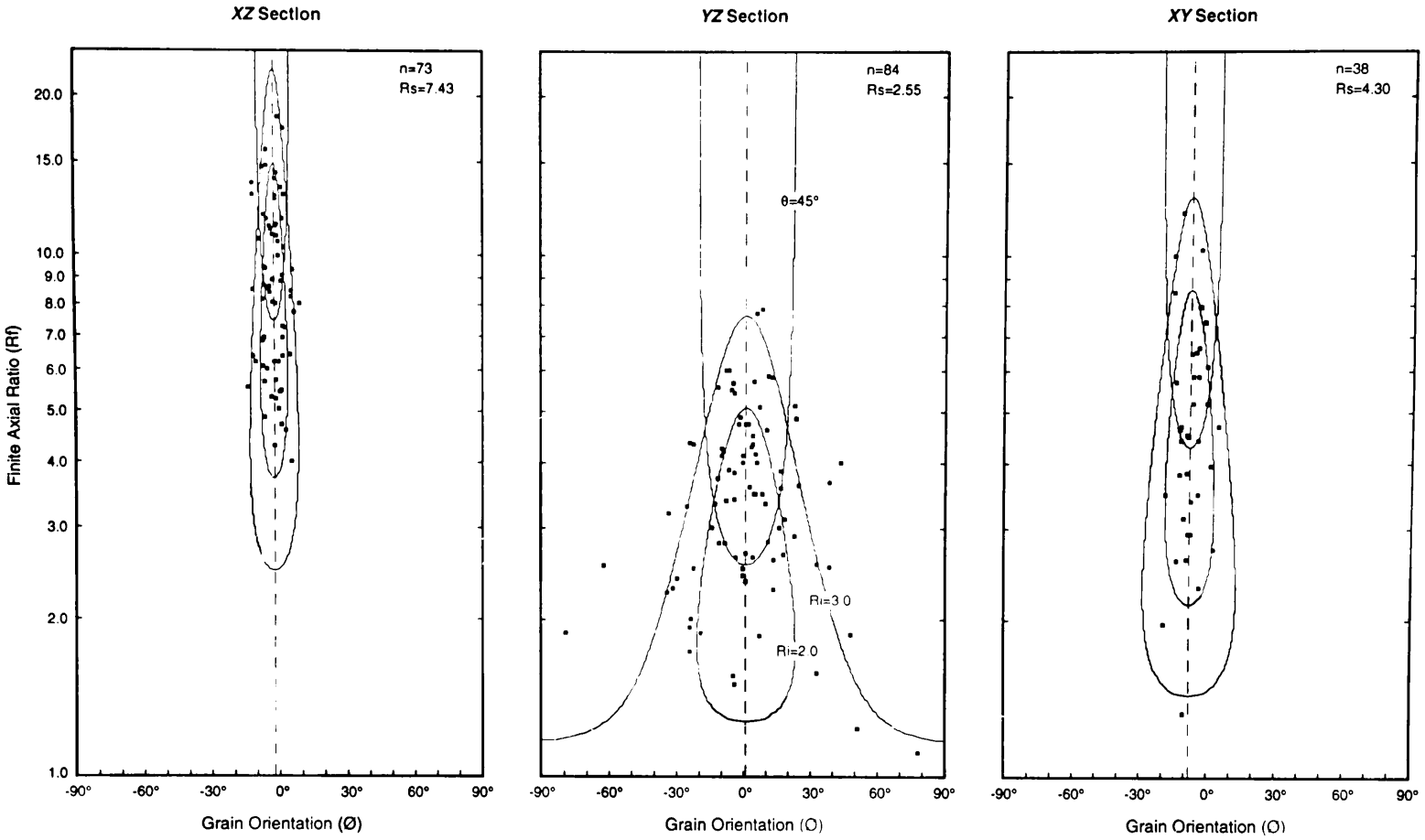

Figure 21. *Rt/Ø* plots for the three principal sections of sample FF62-1. Calculated strain ratio (R_s) indicated in upper right corner of each. R_i and θ curves determined using MACSTRAIN (Kanagawa 1990). See text for discussion.

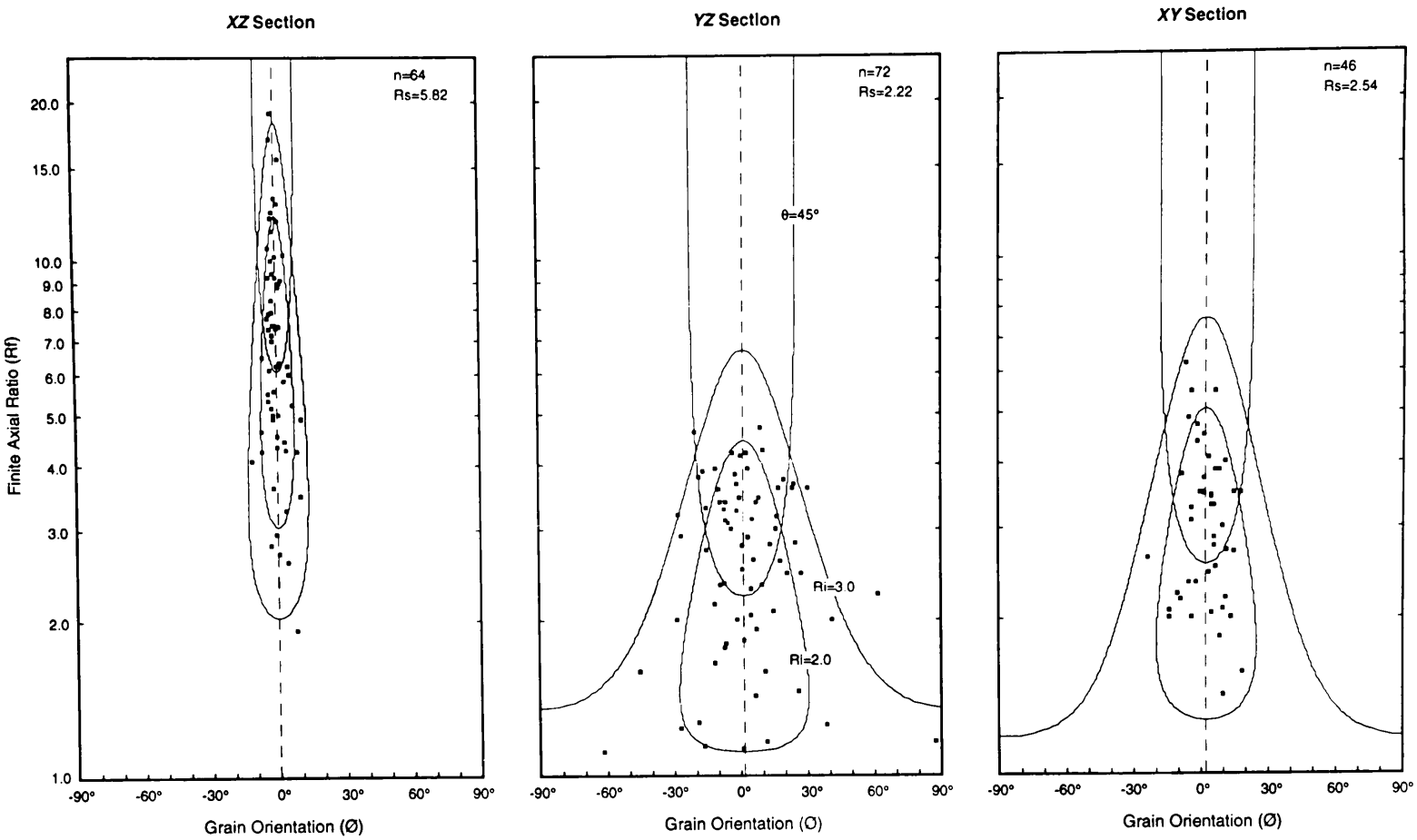

Figure 22. *Rt/Ø* plots for the three principal sections of sample FF78. Calculated strain ratio (R_s) indicated in upper right corner of each. R_i and θ curves determined using MACSTRAIN (Kanagawa 1990). See text for discussion.

Table 1. Axial ratios of deformed detrital quartz grains and finite strain estimates for the principal kinematic sections of Chilhowee Group tectonites.

Sample # →		FF24	FF50	FF62-1	FF78
Rf values*; (sample population)	*XZ*	2.91; (70)	3.63; (73)	7.91; (73)	5.81; (64)
	YZ	2.54; (67)	2.45; (76)	3.04; (84)	2.35; (72)
	XY	1.55; (27)	1.92; (56)	4.07; (38)	2.93; (46)
Rs values†; Rs' (back-calculated)‡	*XZ*	3.03; 2.95	3.61; 3.69	7.43; 10.97	5.82; 5.64
	YZ	2.38; 2.44	2.32; 2.27	2.55; 1.73	2.22; 2.29
	XY	1.24; 1.27	1.59; 1.56	4.30; 2.91	2.54; 2.62
Ri values**	*XZ*	1.78	1.62	2.03	1.78
	YZ	1.67	1.59	2.30	1.91
	XY	1.52	1.76	1.82	1.61

* Harmonic mean (H) of *n* axial ratios (Rf); $H = \left(\frac{n}{\Sigma\left(\frac{1}{Rf}\right)}\right)$

† Strain ratio (Rs) as determined via Rf/Ø analysis in MACSTRAIN 2.0 (Kanagawa 1990)

‡ Back-calculated strain ratio (Rs'); e.g. $Rs'_{(xy)}{}^{\ddagger} = \left(\frac{Rs_{(xz)}{}^{\dagger}}{Rs_{(yz)}{}^{\dagger}}\right)$

** Average initial ellipticities (Ri) as determined via Rf/Ø analysis in MACSTRAIN 2.0 (Kanagawa 1990)

Explanation of symbols used in **Table 2**:

* also includes data compiled from Kaygi (1979) and O'Hara (1990); *XY* ratio adjusted for sample # FF62-1 according to discussion in text

** values calculated on the basis of data presented in reference; *e.g.* under sample "433", $Rs_{(XY)} = [(XZ) / (YZ)]$

Es is the natural logarithmic octahedral strain

$k = [(XY-1) / (YZ-1)]$

$v = [\ln(YZ) - \ln(XY) / \ln(XZ)]$

Table 2. Summary of three-dimensional finite strain data for the Fries fault zone; compiled from analyses of deformed detrital quartz grains (this study) and feldspar grains/augen (Kaygi 1979, O'Hara 1990).

Sample # →		this study				Kaygi (1979)		O'Hara (1990)	
		FF24	FF50	FF62-1	FF78	B	433	VA-4	VA-6
Rs values from Table 1*	*XZ*	3.03	3.61	7.43	5.82	3.91	3.84	2.90**	2.80**
	YZ	2.38	2.32	2.55	2.22	2.44	2.27	2.20	2.50
	XY	1.24	1.59	3.00	2.54	1.45	1.69**	1.30	1.10
X : *Y* : *Z*		1.24 : 1.00 : 0.42	1.59 : 1.00 : 0.43	3.00 : 1.00 : 0.39	2.54 : 1.00 : 0.45	1.45 : 1.00 : 0.41	1.69 : 1.00 : 0.44	1.30 : 1.00 : 0.45	1.10 : 1.00 : 0.40
% extension parallel to *X*, *Y*, and *Z*	*X*	54%	80%	185%	143%	72%	87%	56%	45%
	Y	24%	14%	-5%	-4%	19%	10%	20%	31%
	Z	-48%	-51%	-63%	-57%	-51%	-51%	-46%	-47%
Strain Magnitude (*Es*)		0.811	0.937	1.444	1.225	0.918	0.958	0.781	0.790
Flinn's Parameter (*k*)		0.17	0.45	1.29	1.26	0.31	0.54	0.25	0.07
Lode's parameter (*ν*)		0.59	0.29	-0.08	-0.08	0.38	0.22	0.49	0.80

Figure 23. *Logarithmic Flinn plots of three-dimensional strain data from within the Fries fault zone.*

A. Data from $R_f/\emptyset$ analysis of deformed detrital grains within Chilhowee Group quartzites (filled circles); open circles represent data of Kaygi (1979)*; open triangles based upon strain analysis of O'Hara (1990)*. Also shown are the skeletal outlines of quartz petrofabrics expected for conditions of flattening, plane strain, and constriction (according to Schmid & Casey 1986).

B. *c*-axis petrofabric scatter diagrams corresponding to the samples as shown. See text for discussion, Figure 18 and Appendix 1 for sample localities.

* data based on aspect ratios of felspar grains or augen in various prinicpal sections of Little River Gneiss (Kaygi 1979) and Grayson Gneiss (O'Hara 1990); see Table 2

A.

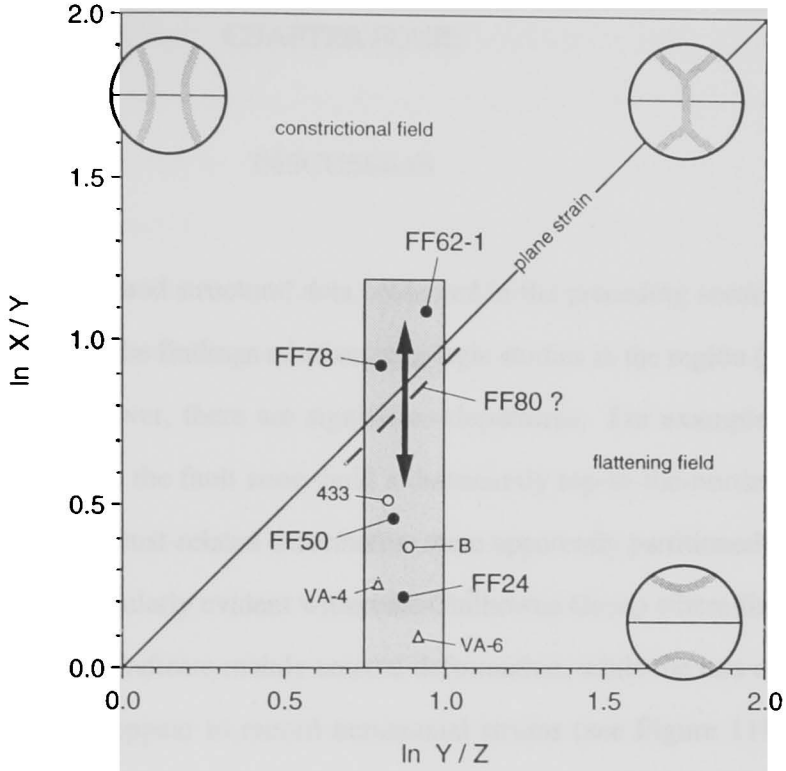
constrictional field
plane strain
FF62-1
FF78
FF80 ?
flattening field
433
FF50
B
VA-4
FF24
VA-6
ln X / Y
ln Y / Z
0.0
0.5
1.0
1.5
2.0

B.

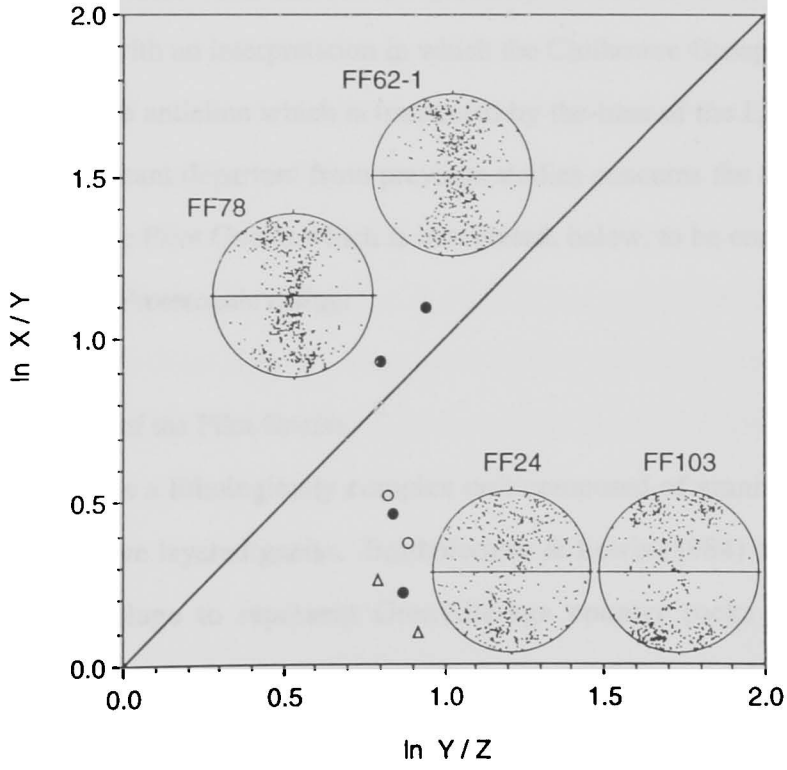
FF62-1
FF78
FF24
FF103
ln X / Y
ln Y / Z
0.0
0.5
1.0
1.5
2.0

CHAPTER FOUR:

DISCUSSION

The map relations and structural data presented in the preceding sections are not entirely inconsistent with the findings of other petrologic studies in the region (*e.g.* Kaygi 1979, Trupe 1989); however, there are significant departures. For example, whereas kinematic analyses within the fault zone yield a dominantly top-to-the-northwest shear sense, the effects of this thrust-related deformation were apparently partitioned according to lithology. This is particularly evident within the Chilhowee Group where finite strains recorded in the quartzites indicate mainly coaxial deformation, while the less competent, phyllosilicate-rich units appear to record noncoaxial strains (see Figure 11B). More importantly, however, the variation in finite strain symmetry and field relations along the fault zone are consistent with an interpretation in which the Chilhowee Group and Pilot Gneiss define an extensive anticline which is transected by the base of the Little River Gneiss. The other significant departure from previous studies concerns the origin and tectonic significance of the Pilot Gneiss which is interpreted, below, to be composed of units associated with Late Proterozoic rifting.

4.1 Tectonic significance of the Pilot Gneiss

The Pilot Gneiss is a lithologically complex unit composed of granitic gneiss, amphibolite, and distinctive layered gneiss. Bartholomew & Lewis (1984) considered the bulk of this assemblage to represent Grenville-age country rocks (possibly metavolcanic) which were metamorphosd at granulite-facies conditions and intruded by granitic magmas later in the Grenville orogeny. However, the only evidence in support

of this interpretation is the reported occurrence of the mineral assemblage: almandine garnet + orthopyroxene in two samples (see Kaygi 1979, Lewis 1975), neither of which were illustrated or referenced to a sample locality. A simpler and more plausible interpretation of the relations documented in this study may be that the layered gneiss complex represents an agglomeration of Late Proterozoic rift-related deposits which were deformed, metamorphosed, and intruded during the early Paleozoic uplift of the Blue Ridge province.

4.1.1 Interpretation of protolith: An alternative to Grenville

Considering the record of dynamothermal metamorphism within the Pilot Gneiss, any interpretation of its protolith is rather tenuous. However, there are several distinctive characteristics which collectively support its origin as a rift-related sequence.

First, the conspicuous compositional layering within the Pilot Gneiss suggests that its protolith *may* have been layered as well. A substantial portion of this stratigraphy is undoubtedly the result of tectonic intercalation and transposition during deformation. Examples of such are recorded by the injection of both mafic and felsic magmas at various times in the deformational history, which are presently oriented parallel to the foliation within the shear zone. Transposition is also evident in the structure of the graphitic schist within the Pilot Gneiss. Exposures of this unit (see Plate 1, also Appendix 1A) sharply transect the predominant structural grain of the layered gneiss complex, although the mylonitic fabrics are nearly concordant at the base of the Pilot Gneiss. More detailed mapping of individual units within the Pilot Gneiss may lead to the recognition of similar structural relationships.

Secondly, the diversity of units found to compose the Pilot Gneiss is not representative of the Grenville basement in adjacent areas (*cf.* Bartholemew & Lewis

1984). Exposures of granoblastic augen gneiss thought to be plutonic in origin, such as the Little River and Grayson gneisses, are more typical of the Grenville in this area. Bartholemew & Lewis (1984) did, however, choose to assign the Pilot Gneiss to the Grenville country rocks, rather than the intrusive suite, although none of the six distinctive units described here contain evidence of the granulite-grade metamorphism which is so characteristic of other layered gneisses in the Grenville terrane. However, it is possible that any record of granulite metamorphism was obliterated during subsequent retrograde events.

Thirdly, it is speculated that the stratigraphic assemblage of units may reflect deposition and modification in a rift-related environment. While there is very little evidence for this, the presence of immature calcareous and feldspathic sands (see sections 2.2.2 and 2.2.4) coupled with widespread sill-like mafic intrusions within the Pilot Gneiss may be interpreted as parts of a rift sequence. Comparable aspects have been documented in a similar, but much less deformed, sequence of rift-related deposits in central Virginia (Wang 1991), although it is difficult to recognize an intact stratigraphy within the Pilot Gneiss .

The final aspect of the Pilot Gneiss which lends support to a rift-related origin concerns its tectonic position relative to younger deposits of the Late Proterozoic rift-drift sequence. In Virginia, the transition from a continental rifting environment to that of a passive continental margin (drift sequence) is recorded within the strata of Chilhowee Group (Simpson & Eriksson 1989). Below this are a series of mafic and felsic volcanic rocks that are locally interstratified with nonmarine clastics (see figure 5b in Glover 1989), collectively interpreted as a part of the Late Proterozoic rift sequence; and speculatively correlated with the Pilot Gneiss. These units are exposed discontinuously along the Blue Ridge front as variably deformed and metamorphosed strata which have

been intercalated along the basement–cover contact. The Pilot Gneiss is situated in a similar tectonic position within the Fries fault zone. In the vicinity of Copper Valley, it is exposed in between the Little River Gneiss and the Chilhowee Group, while elsewhere it is exposed as the core of the Brush Creek anticlinorium and flanked by the Chilhowee Group (Figure 2 and Plate 1). However, these two distinct structural styles may be unified by the field relationships and strain data presented in this thesis, which suggest that the Pilot Gneiss is in the proper structural position for it to be considered as a part of the pre-Chilhowee stratigraphy (see section 4.3).

4.1.2 Taconic signature

As previously stated, this study found no indication of the granulite-grade assemblage which previous workers (*e.g.* Lewis 1975, Kaygi 1979) cited as evidence of Grenville metamorphism. Instead, the results of this investigation suggest that metamorphic conditions in the Pilot Gneiss probably did not exceed the amphibolite facies. This conclusion is based primarily upon the abundance of relict amphibolite layers and hornblende porphyroclasts within the layered gneiss complex, although garnet was also observed in one location near Copper Valley (see section 2.2.6). These phases are the only known record of metamorphic conditions prior to the retrograde, greenschist-facies conditions associated with mylonitization.

Amphibolite-facies metamorphism is recognized throughout the Blue Ridge as an effect of the Taconic orogeny (*ca.* 480-435 Ma, Glover *et al.* 1983), which Kaygi (1979) logically inferred to have affected the Little River and Pilot gneisses. The amphibolites and garnet-bearing rocks of the Pilot Gneiss are interpreted here as having been produced during prograde burial metamorphism of the rift sequence rather than retrograde metamorphism of Grenville basement (*cf.* Bartholemew & Lewis 1984). This, again, is

difficult to substantiate and, although conceivable, relies heavily on how one chooses to interpret the origin of the Pilot Gneiss. Given the Late Proterozoic origin outlined above, the protolith strata would have been buried to a depth of at least 5 to 10 km beneath the passive margin by Early Ordovician time (*ca.* 480 Ma). Further burial during collision with the Taconic terrane would then have led to prograde metamorphism prior to the retrograde deformational conditions recorded within the Fries fault zone.

Unfortunately, there are no reliable absolute ages for the Pilot Gneiss or the metamorphism that has affected it. Dietrich *et al.* (1969) have reported a Rb-Sr whole-rock age of 460 Ma for the Pilot Gneiss which may reflect its primary metamorphism during the Taconic orogeny, although the significance of this age is highly uncertain and may be attributed to either prograde or retrograde metamorphism. Therefore, the possibility of a Grenville protolith remains open to speculation as well.

4.2 Conditions of deformation

The mineralogy and petrology of tectonites in this portion of the Fries fault zone record conditions of greenschist-facies metamorphism associated with northwest-vergent thrusting (*cf.* Kaygi 1979). Mylonitic fabrics are characterized by variable amounts of muscovite, biotite, tremolite, chlorite, epidote, and actinolite, in addition to plastically-deformed and/or recrystallized quartz. This assemblage (within the fault zone as a whole), coupled with the presence of more rigid feldspar porphyroclasts (see section 2.1.1), is considered to indicate that these fabrics were developed at temperatures in the range of 300 to 450°C. Structural analysis of these fabrics indicates that the deformation within the fault zone was strongly noncoaxial and kinematically consistent with the findings of other studies which have revealed northwest-vergent shortening within the Blue Ridge thrust complex (Mies 1988, Trupe 1989, Bailey & Simpson 1993).

Furthermore, the analyses conducted here have shown no compelling evidence of extensional (*i.e.* top-down-to-the-southeast) deformation within the Fries fault zone (*cf.* Simpson & Kalaghan 1989, Bailey & Simpson 1993). However, the results of this study have revealed significant variations in finite strain symmetry along the fault zone which have important implications for its structural evolution.

4.3 Structural framework of the Fries fault zone

Within the area of this study, the Fries fault zone is characterized by two distinct structural styles (see Figure 2 and Plate 1). To the south and east of Riner, VA, the Pilot Gneiss is exposed within the core of the Brush Creek anticlinorium, flanked by the Chilhowee Group, and overridden by the Little River Gneiss; whereas in the vicinity of Copper Valley (to the southwest), the Pilot Gneiss is exposed as a discontinuous sheet in between the Little River Gneiss and Chilhowee Group metasediments. Furthermore, the transition between these structural settings is coincident with a jog in the contact marking the base of the Little River Gneiss. These relations suggest that the Brush Creek anticlinorium (as cored by the Pilot Gneiss) may, in fact, represent only the eastern extent of a more extensive structure which has been transected at various structural levels by the base of the Little River Gneiss.

Finite strain estimates within the Chilhowee Group (see Table 2 and Figure 23) indicate that constrictional–plane strains are focused near the nose of the Brush Creek anticlinorium, whereas flattening strains are more apparent farther southwest (near Copper Valley). The field relationships documented here also show that the Pilot Gneiss is exposed along strike far beyond where it defines the west-plunging Brush Creek anticlinorium. Exposures of the Pilot Gneiss and Chilhowee Group in the vicinity of Copper Valley are thus interpreted to represent a continuation of the same structure,

although only of its overturned northwest limb. Furthermore, the exposure of Pilot Gneiss beyond the apparent plunging termination of the Brush Creek anticlinorium may be used to infer that the hinge line of this structure was depressed in the area where the structural style changes. This interpretation suggests, therefore, that the Brush Creek anticlinorium (and its inferred continuation) existed as a doubly-plunging antiform prior to being transected by the base of the Little River Gneiss, and that the strain associated with emplacement of the Fries thrust sheet was partitioned according to the structure of the footwall. In this case, the finite ductile strain within the Chilhowee Group is thought to be related to thrust emplacement of the Little River Gneiss toward the northwest. As thrusting progressed, an increased gravitational load may have caused flattening and extension of the thrust sheet (see section 3.3), accommodated locally by constrictional–plane strain within structural depressions of the footwall.

While it appears that the development of the Brush Creek anticlinorium preceded the emplacement of the Little River Gneiss (*cf.* Kaygi 1979), it can only be speculated that the folding and thrusting represent progressive stages of the same protracted contractional event. A conceptual model is given below.

Assuming the model of Wehr & Glover (1985) and the possible Late Proterozoic origin for the Pilot Gneiss (outlined in section 4.1.1), the following structural model is proposed for the present structural framework of the fault zone. Northwest-vergent contraction of the continental margin during the Taconic orogeny (*ca.* 480 Ma) initiated burial metamorphism and deformation of Late Proterozoic rift deposits (Figure 24A). Further contraction and generation of kilometer-scale folds adjacent to and within the Blue Ridge thrust complex was accompanied by ductile deformation at greenschist-facies conditions (*cf.* Kaygi 1979, Trupe 1989, Bailey & Simpson 1993). Continued growth of folds and propagation of minor thrusts during uplift may have juxtaposed various

formations of the rift facies (such as the Pilot Gneiss and lower Chilhowee Group strata), although the intensity of deformation obscures these relations. Regardless, the Chilhowee Group was folded along with the Pilot Gneiss to form a doubly-plunging antiform cored by the latter (Figure 24B). Deformation was continually accomodated by general noncoaxial flow, although coaxial strains were effectively partitioned into the more competent quartzite members of the Chilhowee Group, and apparently focused into a structural saddle where the highest strains are recorded (*e.g.* FF62-1 and FF78). The Brush Creek anticlinorium was subsequently transected along its backlimb and through its core by the base of the Little River Gneiss to produce the present-day configuration of units within the Fries fault zone (Figure 24B and C).

Figure 24. *Schematic interpretation for the structural evolution of the Fries fault zone near Riner, Virginia.*

A. Schematic NW-SE cross-section illustrating thrust reactivation of the Laurentian hinge zone during the Taconic orogeny (adapted from Wehr & Glover 1985) leading to intense deformation of the Late Proterozoic rift sequence; abbreviations as in Figure 2 except PGp = Pilot Gneiss protolith.

B. Fries fault (stippled plane, at base of Little River Gneiss) transects the Brush Creek anticlinorium and its implied continuation to the southwest.

C. Schematic illustration of the Fries fault zone in its present state comprising a broad zone of ductile deformation. Core of the Brush Creek anticlinorium preserved only where Little River Gneiss is thrust over the backlimb, while in the vicinity of Copper Valley only the overturned forelimb is exposed. Dashed lines mark the approximate limits of intense ductile deformation and mylonitization along the fault zone. Bold lines represent the major lithologic and structural boundaries of Figure 2. All contacts are interpreted to be tectonic in nature, although the contact between the Chilhowee Group and Pilot Gneiss may represent a modified stratigraphic contact.

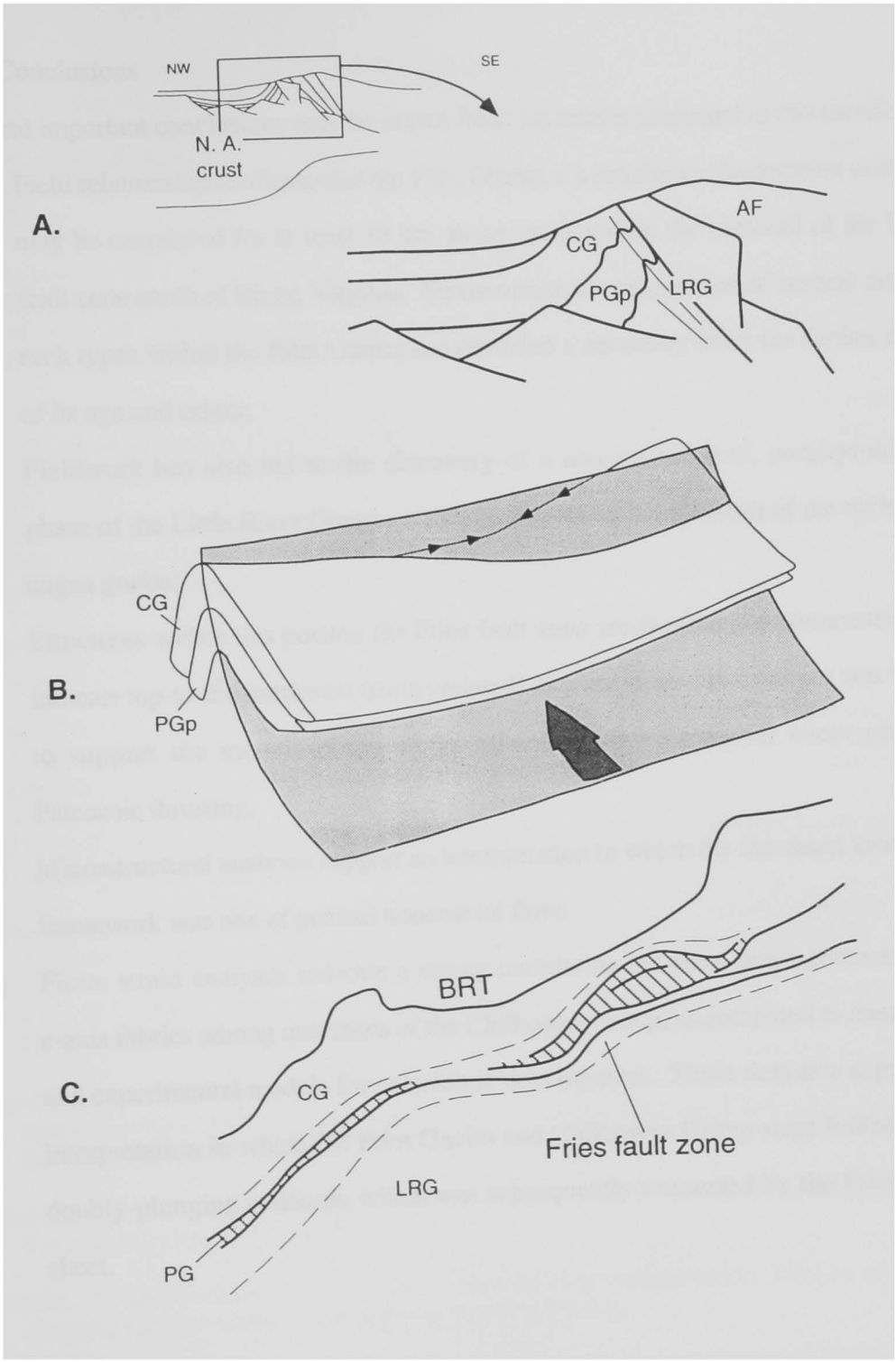
NW
SE
N. A.
crust
A.
AF
CG
PGp
LRG
B.
CG
PGp
BRT
C.
CG
Fries fault zone
LRG
PG

4.4 Conclusions

Several important conclusions may be drawn from the results presented in this thesis:

(1) Field relationships indicate that the Pilot Gneiss is a lithologically complex unit that may be correlated for at least 18 km along strike within the footwall of the Fries fault zone south of Riner, Virginia. Furthermore, the recognition of several distinct rock types within the Pilot Gneiss has provided a necessary basis for further study of its age and origin;

(2) Fieldwork has also led to the discovery of a non-mylonitized, porphyroblastic phase of the Little River Gneiss, which appears to be the protolith of the mylonitic augen gneiss;

(3) Structures within this portion the Fries fault zone are dominantly asymmetric and indicate top-to-the-northwest (thrust-related) displacement. No evidence was found to support the models proposed by others for an extensional event prior to Paleozoic thrusting;

(4) Microstructural analyses support an interpretation in which the dominant kinematic framework was one of general noncoaxial flow;

(5) Finite strain analyses indicate a strong correlation between strain geometry and *c*-axis fabrics among quartzites of the Chilhowee Group, as compared to theoretical and experimental models for petrofabric development. These data also support an interpretation in which the Pilot Gneiss and Chilhowee Group were folded into a doubly-plunging antiform, which was subsequently transected by the Fries thrust sheet.

REFERENCES

Bailey, C.M. & Simpson, C. 1993. Extensional and contractional deformation in the Blue Ridge Province, Virginia. *Geological Society of America Bulletin*, **105**, 411-422.

Bartholomew, M.J. & Lewis, S.E. 1984. Evolution of Grenville massifs in the Blue Ridge geologic province, southern and central Appalachians; *in* Bartholomew, M.J. (editor), The Grenville event in the Appalachians and related topics. *Geological Society of America Special Paper* **194**, 229-254.

Berthé, D., Choukroune, P., & Jegouzo, P. 1979a. Orthogneiss, mylonite and non coaxial deformation of granites: the example of the South Amorican Shear Zone. *Journal of Structural Geology*, **1**, 31-42.

Berthé, D., Choukroune, P., & Gapais, D. 1979b. Orientations préférentielles du quartz et orthogneissification progressive en régime cisaillant: l'exemple du cisaillement sud-amoricain. *Bulletin de Minéralogie*, **102**, 265-272.

Bouchez, J.-L. 1977. Plastic deformation of quartzites at low temperature in an area of natural strain gradient (Angers, France). *Tectonophysics*, **39**, 25-50.

Cook, F.A., Albaugh, D.S., Brown, L.D., Kaufman, S., Oliver, J.E., & Hatcher, R.D. Jr. 1979. Thin-skinned tectonics in the crystalline southern Appalachians; COCORP seismic-reflection profiling of the Blue Ridge and Piedmont. *Geology*, **7**, 563-567.

Dell'Angelo, L.N. & Tullis, J. 1989. Fabric development in experimentally sheared quartzites. *Tectonophysics*, **169**, 1-21.

Dietrich, R.V. 1954. Geology of the Pilot Mountain Area, Virginia. *Bulletin of the Virginia Polytechnic Institute*, Engineering Experiment Station Series No. **91**.

Dietrich, R.V. 1959. Geology and mineral resources of Floyd County. *Bulletin of the Virginia Polytechnic Institute*. Engineering Experiment Station Series No. **134**.

Dietrich, R.V., Fullagar, P.D., & Bottino, M.L. 1969. K/Ar and Rb/Sr dating of tectonic events in the Appalachians of southwestern Virginia. *Geological Society of America Bulletin*, **80**, 307-314.

Dunnet, D. 1969. A technique of finite strain analysis using elliptical particles. *Tectonophysics*, **7**, 117-136.

Dunnet, D. & Siddans, A.W.B. 1971. Non-random sedimentary fabrics and their modification by strain. *Tectonophysics*, **12**, 307-325.

Etchecopar, A. 1977. A plane kinematic model of progressive deformation in a polycrystalline aggregate. *Tectonophysics*, **39**, 121-139.

Etchecopar, A. & Malavieille, J. 1987. Computer models of pressure shadows: a method for strain measurement and shear-sense determination. *Journal of Structural Geology*, **9**, 667-677.

Etchecopar, A. & Vasseur, G. 1987. A 3-D kinematic model of fabric development in polycrystalline aggregates: comparisons with experimental and natural examples. *Journal of Structural Geology*, **9**, 705-717.

Evans, N.H. 1991. Latest Precambrian to Ordovician metamorphism in the Virginia Blue Ridge: Origin of the contrasting Lovingston and Pedlar basement terranes. *American Journal of Science*, **291**, 425-452.

Flinn, D. 1962. On folding during three dimensional progressive deformation. *Geological Society of London Quarterly Journal*, **118**, 385-428.

Glover, L. III. 1989. Tectonics of the Virginia Blue Ridge and Piedmont. *International Geological Conference Field Trip Guidebook* **T363**.

Glover, L. III, Speer, J.A., Russell, G.S. & Farrar, S.S. 1983. Ages of regional metamorphism and ductile deformation in the central and southern Appalachians. *Lithos*, **16**, 223-245.

Hanmer, S. & Passchier, C. 1991. Shear-sense indicators: a review. *Geological Survey of Canada Paper* **90-17**.

Hatcher, R.D. Jr. 1978. Tectonics of the western Piedmont and Blue Ridge, southern Appalachians: Review and speculation. *American Journal of Science*, **278**, 276-304.

Hatcher, R.D. Jr. & Odom, A.L. 1980. Timing of thrusting in the southern Appalachians, USA: model for orogeny? *Journal of the Geological Society of London*, **137**, 321-327.

Jessell, M.W. & Lister, G.S. 1990. A simulation of the temperature dependence of quartz fabrics; in Knipe, R.J. & Rutter, E.H. (editors), Deformation mechanisms, rheology and tectonics. *Geological Society of London Special Publication* **54**, 353-362.

Kanagawa, K. 1990. MACSTRAIN, version 2.0: (A Macintosh-based computer application for determining the symmetry and magnitude of strain), University of Tokyo, Japan.

Karpa, J.B. 1974. The Middle Ordovician Fincastle Conglomerate north of Roanoke, Virignia, and its implications for Blue Ridge tectonism. [*M.S. thesis*]: Virginia Polytechnic Institute and State University.

Kaygi, P.B. 1979. The Fries fault near Riner, Virginia: An example of a polydeformed, ductile deformation zone. [*M.S. thesis*]: Virginia Polytechnic Institute and State University.

Kirschner, D. & Teyssier, C. 1991. Quartz c-axis fabric differences between porphyroclasts and recrystallized grains. *Journal of Structural Geology*, **13**, 105-109.

Lampshire, L.D., Çoruh, C. & Costain, J.K. 1994. Crustal structures and the eastern extent of lower Paleozoic shelf strata within the central Appalachians: A seismic relection interpretation. *Geological Society of America Bulletin*, **106**, 1-18.

Law, R.D. 1986. Relationships between strain and quartz crystallographic fabrics in the Roche Maurice quartzites of Plougastel, western Brittany. *Journal of Structural Geology*, **8**, 493-515.

Law, R.D. 1987. Heterogeneous deformation and quartz crystallographic fabric transitions: natural examples from the Stack of Glencoul, northern Assynt. *Journal of Structural Geology*, **9**, 819-833.

Law, R.D. 1990. Crystallographic fabrics: a selective review of their applications to research in structural geology; *in* Knipe, R.J. & Rutter, E.H. (editors), Deformation mechanisms, rheology, and tectonics. *Geological Society of London Special Publication* **54**, 335-352.

Law, R.D., Casey, M. & Knipe, R.J. 1986. Kinematic and tectonic significance of microstructures and crystallographic fabrics within quartz mylonites from the Assynt and Eriboll regions of the Moine thrust zone, NW Scotland. *Transactions of the Royal Society of Edinburgh: Earth Sciences*, **77**, 99-125.

Law, R.D., Knipe, R.J. & Dayan, H. 1984. Strain path partitioning within thrust sheets: microstructural and petrofabric evidence from the Moine thrust zone at Loch Eriboll, northwest Scotland. *Journal of Structural Geology*, **6**, 477-497.

Law R.D. & Potts, G.J. 1987. The Tarskavaig nappe of Skye, northwest Scotland: a re-examination of the fabrics and their kinematic significance. *Geological Magazine*, **124**, 231-248.

Lewis, S.E. 1975. Geology of the southern part of the Riner quadrangle, Montgomery and Floyd counties, Virginia. [*M.S. thesis*]: North Carolina State University.

Lister, G.S. 1977. Discussion: Crossed girdle c-axis fabrics in quartzites plastically deformed by plane strain and in progressive simple shear. *Tectonophysics*, **39**, 51-54.

Lister, G.S., Paterson, M.S., & Hobbs, B.E. 1978. The simulation of fabric development during plastic deformation and its application to quartzite: the model. *Tectonophysics*, **45**, 107-158.

Lister, G.S. & Hobbs, B.E. 1980. The simulation of fabric development during plastic deformation and its application to quartzite: the influence of deformation history. *Journal of Structural Geology*, **2**, 355-370.

Lister, G.S. & Snoke, A.W. 1984. S-C mylonites. *Journal of Structural Geology*, **6**, 617-638.

Lister, G.S. & Williams P.F. 1979. Fabric development in shear zones: theoretical controls on observed phenomena. *Journal of Structural Geology*, **1**, 283-297.

Lister, G.S. & Williams P.F. 1983. The partitioning of deformation in flowing rock masses. *Tectonophysics*, **92**, 1-33.

Mancktelow, N. 1989. STEREOPLOT, version 1.2: (A plotting program for oriented data using the Macintosh computer), Geologisches Institut, ETH, Zurich, Switzerland.

Marjoribanks, R.W. 1976. The relation between microfabric and strain in a progressively deformed quartzite sequence from central Austrailia. *Tectonophysics*, **32**, 269-293.

McDowell, R.C. 1968. Structural geology of the Macks Mountain area Virginia. [*M.S. thesis*]: Virginia Polytechnic Institute and State University.

Means, W.D. 1981. The concept of steady-state foliation. *Tectonophysics*, **78**, 179-199.

Mies, J.W. 1988. A major thrust at the base of the Ashe Formation in the Blue Ridge of northwestern North Carolina. *Geological Society of America Abstracts with Programs*, **20**, 280.

O'Hara, K. 1990. State of strain in mylonites from the western Blue Ridge province, southern Appalachians: the role of volume loss. *Journal of Structural Geology*, **12**, 419-430.

Passchier, C. 1991. Geometric constraints on the development of shear bands in rocks. *Geologie en Mijnbouw*, **70**, 203-211.

Passchier, C. & Simpson, C. 1986. Porphyroclast systems as kinematic indicators. *Journal of Structural Geology*, **8**, 831-843.

Platt, J.P. & Behrmann, J.H. 1986. Structures and fabrics in a crustal-scale shear zone, Betic Cordillera, SE Spain. *Journal of Structural Geology*, **8**, 15-33.

Platt, J.P. & Vissers, R.L.M. 1980. Extensional structures in anisotropic rocks. *Journal of Structural Geology*, **2**, 397-410.

Price, G.P. 1985. Preferred orientations in quartzites; *in* Wenk, H.-R., editor, Preferred orientations in deformed metals and rocks: an introduction to modern texture analysis. Academic Press, New York. 385-406.

Ramsay, J.G. 1980. Shear zone geometry: a review. *Journal of Structural Geology*, **2**, 83-99.

Ramsay, J.G. & Graham, R.H. 1970. Strain variation in shear belts. *Canadian Journal of Earth Sciences*, **7**, 786-813.

Rankin, D.W., Espenshade, G.H., & Wier Shaw, K. 1973. Stratigraphy and structure of the metamorphic belt in northwestern North Carolina and southwestern Virginia: A study from the Blue Ridge across the Brevard fault zone to the Sauratown Mountains anticlinorium. *American Journal of Science*, **273-A**, 1-40.

Schmid, S.M. & Casey, M. 1986. Complete fabric analysis of some commonly observed quartz c-axis patterns; *in* Hobbs, B.E. & Heard, H.C., editors, Mineral and Rock Deformation: Laboratory Studies. *American Geophysical Union Monograph*, **36**, 263-286.

Simpson, C. & Kalaghan, T. 1989. Late Precambrian crustal extension preserved in Fries fault zone mylonites, southern Appalachians. *Geology*, **17**, 148-151.

Simpson, E.L. & Eriksson, K.A. 1989. Sedimentology of the Unicoi Formation in southern and central Virginia: Evidence for Late Proterozoic to Early Paleozoic rift-to-passive margin transition. *Geological Society of America Bulletin*, **101**, 42-54.

Stose, A.J. & Stose, W.S. 1957. Geology and mineral resources of the Gossan Lead district and adjacent areas in Virginia. *Virginia Division of Mineral Resources Bulletin*, **72**.

Teyssier, C., Amri, C., & Hobbs, B.E. 1988. South Arunta Block: the internal zones of a Proterozoic overthrust in central Austrailia. *Precambrian Research*, **40-41**, 157-173.

Truman, W.E. III. 1976. Geology of the Blue Ridge Front near Riner, Virginia. [*M.S. thesis*] Virginia Polytechnic Institute and State University.

Trupe, C.H. III. 1989. Microstructural analysis of mylonites from the Blue Ridge thrust complex, western North Carolina. [*M.S. thesis*]: University of North Carolina at Chapel Hill.

Tullis, J. 1977. Preferred orientation of quartz produced by slip during plane strain. *Tectonophysics*, **39**, 87-102.

Tullis, J. 1983. Deformation of feldspars; *in* Ribbe, P.H. (editor), Feldspar Mineralogy. *Reviews in Mineralogy*, **2**, 297-322.

Tullis, J., Christie, J.M., & Griggs, D.T. 1973. Microstructure and preferred orientations of experimentally deformed quartzites. *Geological Society of America Bulletin*, **84**, 297-314.

Wang, P. 1991. Geology and tectonic significance of the late Precambrian Blue Ridge cover sequence in central Viriginia. [Ph.D. dissertation]: Virignia Polytechnic Institute and State University.

Wehr, F. & Glover, L., III. 1985. Stratigraphy and tectonics of the Virginia-North Carolina Blue Ridge: evolution of a late Proterozoic hinge zone. *Geological Society of America Bulletin*, **96**, 285-295.

White, S.H. 1973. The dislocation structures responsible for the optical effects in some naturally deformed quartzites. *Journal of Material Science*, **9**, 490-499.

White, S.H., Burrows, S.E., Carreras, J., Shaw, N.D., & Humphreys, F.J. 1980. On mylonites in ductile shear zones. *Journal of Structural Geology*, **2**, 175-187.

APPENDIX 1

Outcrop and sample localities referenced according to specimen number and/or figure number listed in text. Base map areas are outlined on Plate 1.

Appendix 1A: Copper Valley region

Appendix 1B: Pilot region

Explanation of symbols used in Appendix 1:

▲	photograph shown in thesis
②	site referred to in thesis (see Chapter 2, also Plate 1)
⇄	meso-to-microstructural shear-sense indicator documented in thesis (includes *only* those samples discussed in text)
✳	quartz *c*-axis petrofabric diagram illustrated in thesis
⌀	$R_f/\emptyset$ strain data presented in thesis

Appendix 1A

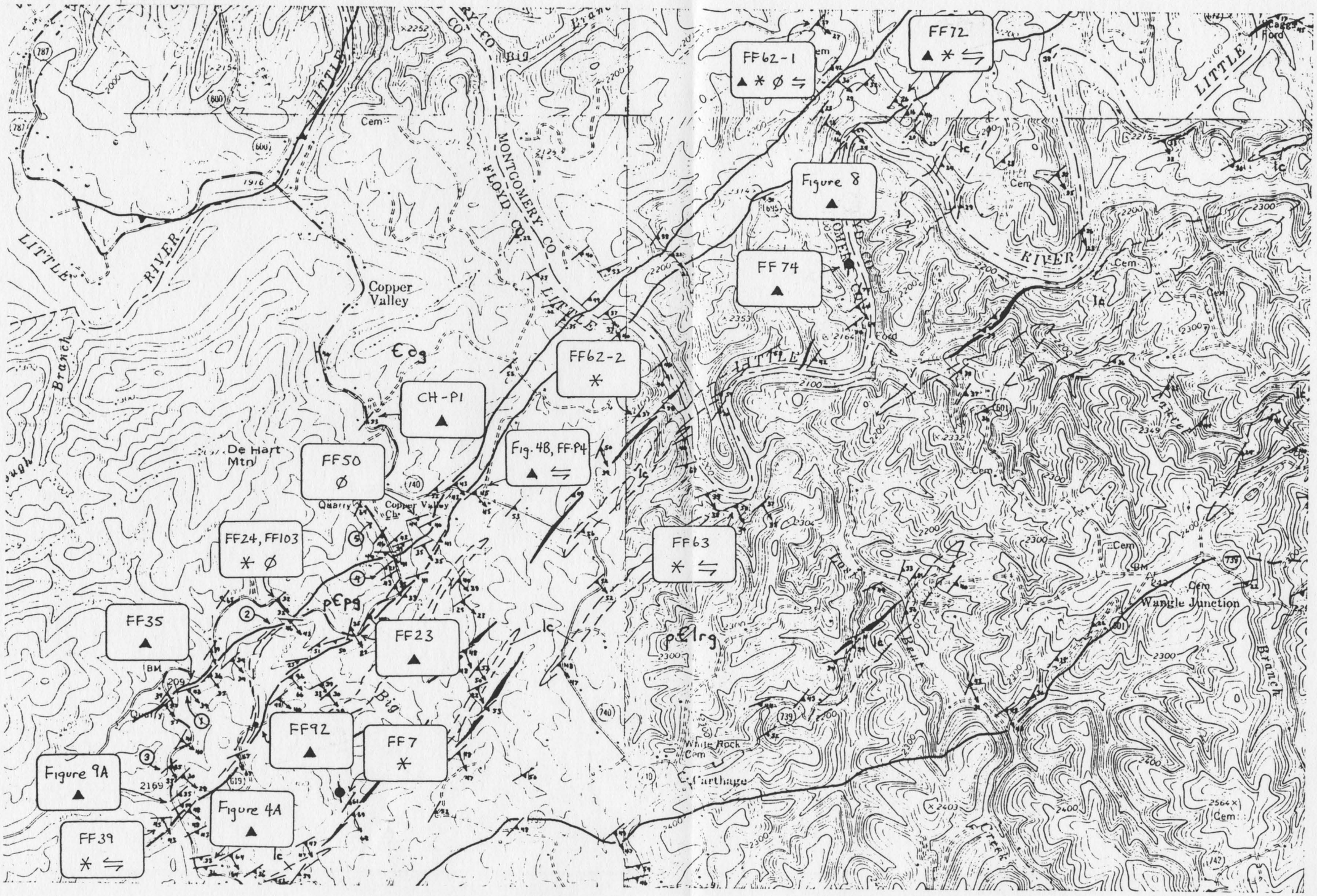
FF72
FF62-1
Figure 8
FF74
FF62-2
CH-P1
Fig. 4B, FF-P4
FF50
FF24, FF103
FF35
FF23
FF92
FF7
Figure 9A
FF39
Figure 4A
FF63
LITTLE RIVER
Copper Valley
De Hart Mtn
Quarry
Cem
Big Branch
Wangle Junction
White Rock Cem
Carthage
Ford
MONTGOMERY CO.
FLOYD CO.

Appendix 1B

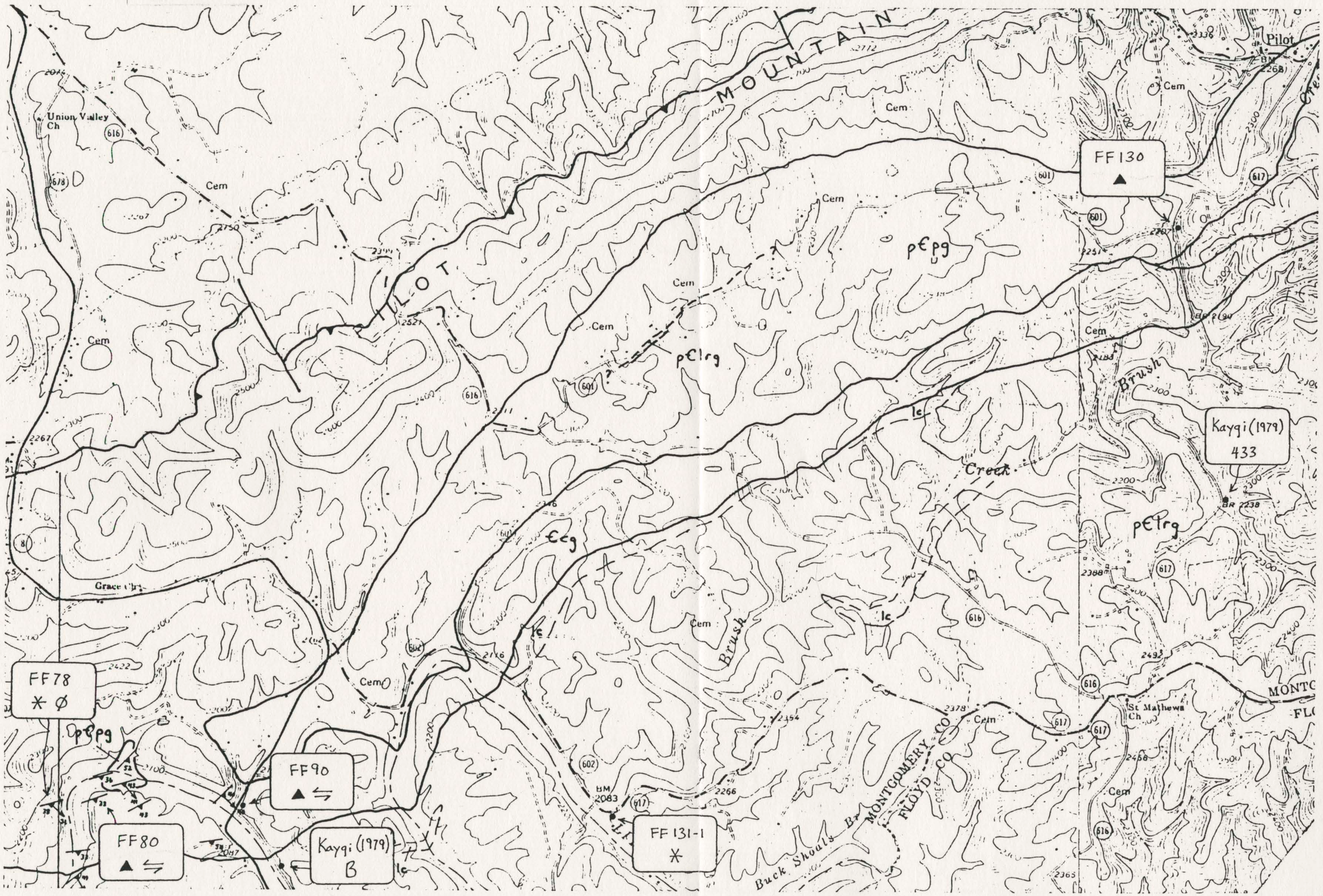
PILOT MOUNTAIN
Union Valley Ch
Cem
Grace Ch
FF130
Kayqi (1979) 433
FF78
FF80
FF90
Kayqi (1979) B
FF 131-1
p€pg
p€lrg
€cg
lc
Brush Creek
Buck Shoals Br
MONTGOMERY CO
FLOYD CO
St Mathews Ch
Pilot

VITA

Richard Sawyer Whitmarsh was born in Brockton, Massachusetts on May 5, 1966. After graduating from East Bridgewater High School (Mass.) in 1984, he attended the University of North Carolina at Charlotte where he earned his Bachelor's degree. In the Fall of 1989, Richard began his research toward a Master's degree in structural geology at Virginia Tech, during which he participated in British Petroleum's Summer Intern Program located in Anchorage, Alaska (1991) and Houston, Texas (1992). He is currently working toward a Doctoral degree at the University of Kansas.